Capacitive Displacement Sensing for the Nanogate
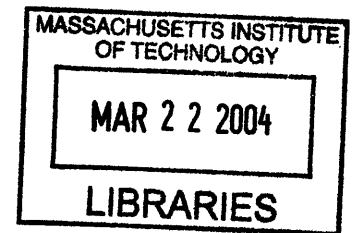
by

Hongshen Ma

B.A.Sc. University of British Columbia (2001)

Submitted to the Program in Media Arts and Sciences,
School of Architecture and Planning,
In partial fulfillment of the requirements for the degree of

Masters of Science in Media Arts and Sciences

at the

MASSACHUSETTS INSTITUTE OF TECHNOLOGY

February 2004

Author_____
Program in Media Arts and Sciences
January 15, 2004

Certified by_____
Joseph A. Paradiso
Associate Professor
Sony Career Development Professor of Media Arts and Sciences
MIT Program in Media Arts and Sciences

Accepted by_____
Andrew Lippman
Chair, Department Committee on Graduate Students
MIT Program in Media Arts and Sciences

Abstract

The Nanogate is a micro electro mechanical systems (MEMS) device that uses a cantilever structure to control the separation between two extremely flat surfaces. It has been proposed that the Nanogate be used as part of a nanoscale instrument for studying the behavior of fluids at the molecular scale. This thesis describes the development of an integrated capacitive displacement sensor which enables nanometer precision measurement of the separation of the surfaces of the Nanogate.

The work in this thesis can be divided into two parts: fabrication of a new version of the Nanogate and the development of electronics for the capacitive sensor. The fabrication part involved redesigning the Nanogate package and fabrication process to integrate the capacitive sensing electrodes, as well as to improve the process yield. The development of capacitive sensing electronics for the Nanogate involved the design of an analog front-end to convert capacitance to voltage and a custom high precision data acquisition system to digitize the output.

The measured capacitance is converted back to absolute displacement by calibration with a Michelson interferometer-based displacement sensor. The results show a resolution better than 0.1nm and the long term drift error is less than 1nm.

Capacitive Displacement Sensing for the Nanogate

by

Hongshen Ma

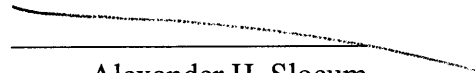The following people served as readers for this thesis:

Thesis Reader_____

Joseph A. Paradiso

Associate Professor

Sony Career Development Professor of Media Arts and Sciences

MIT Program in Media Arts and Sciences

Thesis Reader_____

Alexander H. Slocum

Professor

MacVicar Faculty Fellow

MIT Department of Mechanical Engineering

Thesis Reader_____

Scott R. Manalis

Assistant Professor

NEC Career Development Professor of Computers and Communications

MIT Program in Media Arts and Sciences

Acknowledgements

To my supervisor, **Joe Paradiso**, for bringing me to the lab, for helping me to grow as an engineer and as a person, for having the understanding to let me take on this project, and for supporting me until the very end. You taught me to be relentless in quest for the answer; and then you taught me about humility and kindness in everything else. To you I am deeply indebted.

To **Alex Slocum** for always being optimistic, for treating his students like family, and for always making research fun.

To **Scott Manalis** for the early discussions in the Silicon Biology class.

To **James White** for teaching me everything I know about MEMS fabrication.

To **Ari Benbasat** for being a great friend and for working with me on my writing every step of the way.

To **Stacy Morris** for always bringing a smile to the lab.

To **Mat Laibowitz** for his help with the microprocessor work and for being a messy, but wonderful officemate.

To the **Responsive Environments Group** for making the lab a great place to work and play.

To **Kurt Broderick, Gwen Donahue**, and the rest of MTL staff for their generous help with the fabrication process.

To **Kaity Ryan** for the last minute corrections.

To the **Natural Sciences and Engineering Research Council** of Canada for their financial support.

Finally, to **my parents** and my best friend, **Chris Qually**, for reminding me to work hard even when I didn't want to and for always having faith in me along the way.

Table of Contents

List of Figures

List of Tables

1 Introduction

The study of the physical properties of fluids at the molecular scale has gathered considerable research interest. Numerous studies have shown that as the sample size is reduced, bulk models often break down, yielding to a regime where the molecular nature of the fluid must be considered [1-4]. As these studies converge to the length scale of an individual molecule, which is on the order of nanometers, there is a need for instruments that can confine and measure materials at this new level of precision.

The Nanogate is a micro electro mechanical systems (MEMS) device that uses a cantilever structure to control the separation between two ultra-flat surfaces. Using MEMS materials and processing techniques, it is possible to fabricate devices with nanometer-scale smooth surfaces. It is therefore possible to build a tunable gap with nanometer order size and precision. In a gap from a few to tens of nanometers wide, it is hypothesized that fluid can enter a regime where molecular behavior dominates over bulk behavior [1-4]. Consequently, the Nanogate could form the basis of an instrument to 1) study the mobility of molecules in a fluid as a way to separate the species of interest; or 2) measure the electrical response of molecules as a means of identifying the species of interest.

The work in this thesis is intended to be an initial step towards this nanometer scale instrument by developing a displacement sensor to accurately measure the size of the nanometer gap. Specifically, this involves fabricating a new version of the Nanogate and developing the necessary electronic instrumentation to produce a digital readout that can be used for servo control.

1.1   Basic Principle

Professor Alexander Slocum and James White at MIT's Mechanical Engineering Department initially conceived the concept of the Nanogate [5-7]. The Nanogate is fabricated at MIT's Microsystems Technology Laboratory (MTL) using photolithography and surface micromachining techniques. Its basic structure consists of a disc-shaped silicon diaphragm assembled together with a Pyrex diaphragm that forms a circular lever-

fulcrum structure, where the size off the center gap can be varied by applying a force to the outer edge.
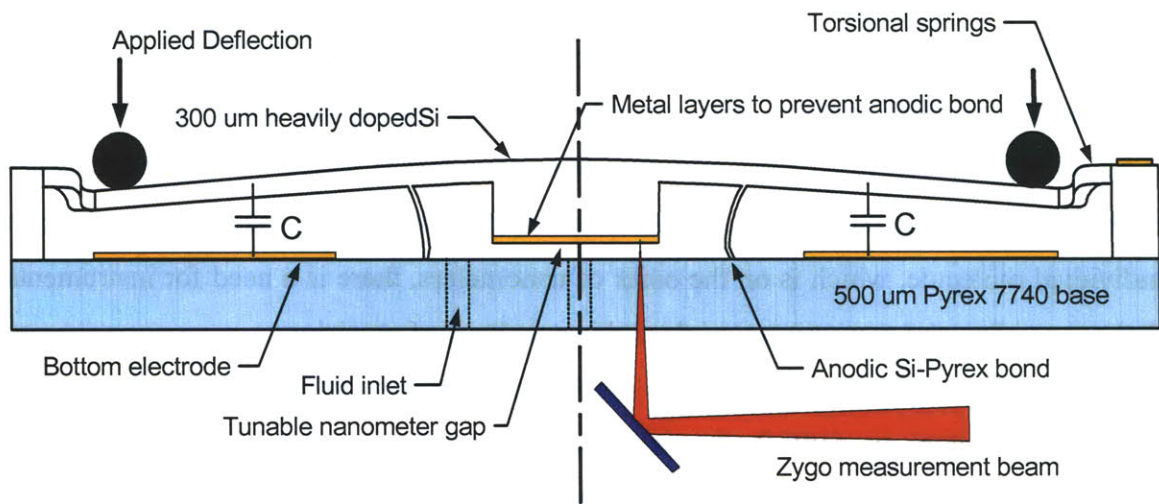
Figure 1: Cross section of the Nanogate with Added Capacitive Sensor Electrodes
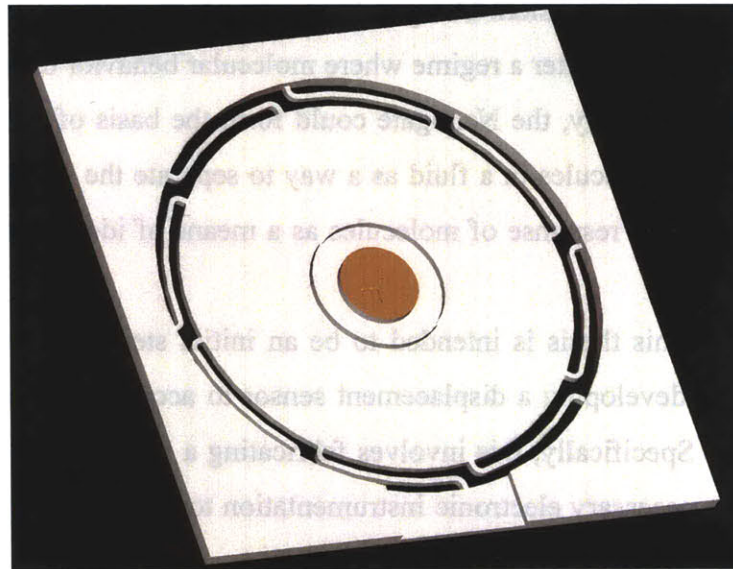
Figure 2: CAD model of the Nanogate silicon diaphragm

Figure 1 show a cross section of this structure where the axis of revolution runs through the center. The top half of the device is made of a micromachined silicon wafer shown in Figure 2. The central disc, known as the valveland (Figure 2), is where the smooth silicon surface makes intimate contact with its corresponding Pyrex surface. This area is deposited with metal layers which prevent bonding with the Pyrex base. Concentric with the valveland is a ring protrusion that is anodically bonded to the Pyrex

16

glass to form a circular fulcrum. When a force is applied to the outer edge of the silicon disc, the flex of the fulcrum determines the mechanical transmission ratio from outer edge to the valveland. This mechanical advantage serves to magnify the mechanical impedance of the central valveland, and similarly, precision control of gap. Flexible spring elements are also machined into the silicon diaphragm to hold the disc in place during the fabrication process.

1.2 Key Characteristics of the Nanogate

The structure of the Nanogate yields several important characteristics. First, the surface roughness of standard silicon and Pyrex wafers is 2-3 nanometers and can be reduced to less than 0.3 nanometers through specialized polishing techniques. By preserving this surface finish throughout the fabrication process, it is possible to produce a true, parallel nanometer gap. As additional evidence will show, the anodic bonding process causes the Pyrex wafer to reflow to the shape of the silicon layer, making the two surfaces complementary to each other.

Second, the gap is adjustable with a large dynamic range, from a few nanometers to micrometers. This property can be used in a precision fluid control system where the flow rate can be precisely tuned. Furthermore, when clogging occurs in a small channel, the valve can be opened a large amount to flush the channel.

Third, the stiffness of single crystalline silicon and the silicon-to-Pyrex anodic bond give the valveland region tremendous mechanical impedance. This is further magnified by the mechanical transmission provided by the lever-fulcrum structure. As a result, it is possible to control the gap distance independent of materials and surface forces in the gap.

Fourth, the design of the Nanogate allows for a large lateral dimension relative to the gap dimension. This provides a large surface area to volume ratio for chromatography applications where it is beneficial to maximize the interaction between the fluid and channel surfaces.

Finally, the Pyrex-silicon chamber formed by anodic bond is vacuum tight, which means that the Nanogate could be used as a valve in gas applications where a vacuum

seal is required. In fact, it has been shown that the Nanogate device has one of the lowest helium-leak rates among available microvalves [7].

1.3 Previous work

James White designed the original structure of the Nanogate and developed a process to fabricate these devices at MTL as part of his Ph.D. work [7]. The original design has a 1.5mm diameter valveland and 2.25mm diameter fulcrum. The outer diameter of the disc is 7.5mm and the designed transmission ratio from the deflection of the outer edge to the gap is 15:1. The entire silicon die is a 10 x 10 mm square fabricated on a 100 mm diameter silicon wafer. The individual dies are separated using a diesaw and then bonded to a Pyrex base of the same dimensions.

In the fall of 2001, White and Ma designed an experimental fixture to test the initial version of the Nanogate. The Nanogate is actuated through a spring flexure using a piezoelectric motor. The piezoelectric motor drove a lead screw that advanced in submicron steps. The displacement of the center region is measured using a commercial Michelson interferometer made by Zygo [8]. These experiments showed controlled displacement of the center region in 2.4nm steps [9].

Although the original device and experiment showed great promise, there are several problems that hinder its ability to achieve nanometer control of the gap size. The Zygo interferometer used to measure displacement had drift problems on the order of 100nm per hour, which makes impractical to use for feedback control on the nanometer level. Additionally, the Zygo is bulky and expensive instrument that would be impractical for widespread use.

Another problem is the unreliable results produced from the original fabrication process. Since the silicon and Pyrex diaphragm are bonded as individual dies rather than entire wafers, the wafers had to be cut before proceeding with the anodic bond. Particles from the diesawing process often contaminated the bonding surfaces and drastically reducing the yield of successful devices. Furthermore, even before the diesaw, the bond surfaces are often already contaminated in the previous micromachining step where photoresist is an insufficient masking material.

18

1.4 Thesis Goals and Specifications

The goal of this work is to develop a displacement sensor to allow the Nanogate to more accurately and easily measure the size of the gap at the valveland. The specifications include measurement of the gap size to better than 1nm with long term drift error less than 1nm. In addition to providing a more accurate measurement, this displacement sensor must also be compatible with fluid based experiments and mechanically integrateable with the Nanogate's external actuator. This development process involves first deciding on a displacement measurement strategy, then fabricating a new version of the Nanogate that integrates the features necessary for measurement, and finally developing the supporting instrumentation that can provide an electronic readout. Compared to the bulky interferometer used previously, a simpler and more compact measurement system is desired.

The development of the displacement sensor for the Nanogate initially involves choosing a sensing strategy. This process is described in Chapter 2 and concludes with the decision to use capacitive sensing. Next, an improved fabrication process, designed to incorporate the capacitive sensor, is presented in Chapter 3. This chapter also includes the characterization of the fabricated components. The development of electronics for measuring capacitance sensing is discussed in Chapter 4. This section includes descriptions of the capacitive sensing front end, analog signal conditioning, precision data acquisition system, and the computer control interface as well as the PCB design. Results from the capacitive displacement sensing are presented in Chapter 5 along with analysis of noise and drift in the system. This thesis concludes in Chapter 6 where possible improvements on the system and future work are discussed.

2 Displacement Sensor Design

This section begins with a presentation of the displacement sensing modalities appropriate for measuring position with nanometer accuracy. Then, the strengths and weaknesses of each sensor are weighed in the context of sensing for the Nanogate. Finally, a detailed design of the capacitive displacement sensor for the Nanogate is presented.

2.1 Displacement Sensing Modalities

A variety of sensing modalities are available to measure position with nanometer resolution including techniques that measure optical intensity, optical phase, capacitance, magnetic field, and piezoelectric response. Piezoelectric sensors [10, 11] are quickly dismissed because of poor repeatability and excessive temperature sensitivity; Magnetic field sensors [11] are also eliminated because of susceptibility to interference and difficulty in integration into the Nanogate fabrication process. The others merit further examination.

Optical intensity-based displacement sensors measure the change in amplitude of a light beam reflected off the target of interest. The most accurate of this type of sensor reflects off the target at an angle and then uses a CCD array to triangulate the position of the reflected spot. By assuming a Gaussian beam and then interpolating between CCD elements, sub-wavelength accuracy can be achieved. Keyence sells a commercial version of this displacement sensor with 10nm resolution with 20 kHz bandwidth [12].

Optical phase based position sensors use a laser source to generate a diffraction pattern. The change in the diffraction pattern as a function of position can then be measured using a photodetector. Two realizations of this general technique are the Michelson interferometer and interdigitated diffraction gratings. The Michelson interferometer uses light from a laser source and divides it into two beams. Each beam travels a separate path and is reflected back via a retro-reflector to recombine and form a standing wave interference pattern. Usually, the path length of one beam is fixed and is

considered to be the reference path while the path length of the other beam is variable and is considered to be the measurement path. The phase of the interference pattern is depended on the phase difference of the two paths. By measuring the amplitude at a specific point along the interference pattern it is possible to determine the displacement to a fraction of the wavelength of the source. Zygo makes a commercial version of this instrument where displacement can be measured with up to 2.4nm resolution at 4 kilo-samples-per-second [8]. An optional attachment of this instrument allows the measurement beam to be focused off a planar reflector target instead of using a retro-reflector [13]. This configuration is used to measure displacement in the first incarnation of the Nanogate where the beam is focused through the Pyrex base at the valveland. One of the problems with this setup is that the measurement is non-differential. It is prone to thermal drift in the mechanical structure, which is measured to be on the order of 100nm per hour [9].

Interdigitated diffraction gratings use two gratings offset by half of their period to form a grating with double the frequency. The grating is excited by a laser source, which forms a diffraction pattern. Moving gratings out of plane with respect to each other modulates the antinodes of the odd and even harmonic in the diffraction pattern. Using a split photodiode pair to measure the difference over sum of the adjacent antinodes, it is then possible to measure the motion of the gratings with extreme precision. Manalis et al have shown displacement measurements with resolution down to 0.002 nanometers with a 1kHz bandwidth [14, 15].

Capacitive sensors electronically measure the capacitance between two or more electrodes and convert this value to a displacement [16-19]. The usual technique involves exciting the measurement capacitor at a high frequency and then measuring its impedance response. The high frequency excitation reduces the impedance of the capacitor to a manageable range and the response signal is down-converted to a DC voltage. Capacitive sensors are used extensively for position sensing in MEMS devices. Perhaps one of the most successful commercial products is the ADXL series accelerometers from Analog Devices, which use capacitance to measure the motion of a tethered proof mass. The ADXL series devices uses entirely integrated electronics and have demonstrated better than 0.002 nanometer resolution position sensing with a bandwidth of 10 kHz [18, 20].

2.2 Choice of Displacement Sensing Strategy

Method	Resolution	Drift	Bandwidth	Integration Requirements
Laser intensity – triangulation with CCD [12]	10 nm	40 nm/C	20 kHz	Optical path to the Nanogate
Michelson interferometer [8, 13]	2.4 nm	100 nm/hr	20 kHz	Optical path to the Nanogate
Interdigitated gratings [14, 15]	0.002 nm	N/A	1 kHz	Optical path to the Nanogate and fabricated grating features.
Capacitive measurement [18, 20]	0.002 nm	N/A	10 kHz	Two electrodes and wire connection

Table 1: Modalities for nanoscale displacement sensing

Resolution, drift, and ease of integration with the Nanogate are considered in choosing the displacement sensing technology. Table 1 summarizes the relevant specifications of the different sensing modalities. The target resolution is 1nm, at 100Hz bandwidth, with less than 1nm/hour of drift.

The intensity-based position sensor is dismissed due to lack of resolution. The Zygo interferometer has borderline acceptable resolution, but the nature of this measurement scheme also leads to problems with drift. Additionally, the Zygo is a bulky and expensive setup and not practically for wide use of the Nanogate.

The interdigitated diffraction grating sensor is an intriguing possibility because it is a true differential measurement. However, in order to integrate this sensing scheme, gratings must be embedded in the Pyrex at some fixed depth away from the Pyrex-silicon interface. This is a challenging task as well-controlled etching of Pyrex is not an established technique at MTL.

The capacitive sensors can be designed with extremely high resolution and would be simple to integrate with the Nanogate. Therefore, it is the choice of displacement sensing for this work. The disadvantage of capacitive sensing is that it is difficult to translate a change in capacitance to an absolute displacement. This difficulty arises due the presence of stray coupling of electric fields (e.g. stray capacitance), which is a

difficult parameter to model and predict in a complicated geometry such as the Nanogate with external connections. Therefore, a calibration routine is necessary to determine the capacitance to displacement mapping.

2.3   Capacitive Sensor Design

The most straightforward approach to Nanogate displacement sensing via capacitance would have been to put electrodes on either sides of the gap. However, the impedance measurement would depend on the dielectric and conductive properties of the liquid or gas in the gap. To avoid this problem, the capacitive measurement is made at the outside edge of the cantilever, with the silicon diaphragm as one electrode and a gold trace deposited on the Pyrex as the other electrode (Figure 3). It is assumed that deflection around the outside edge has a single-valued and stable mapping to the movement of the valveland. This is a reasonable assumption because a single crystal silicon wafer has no mechanism for creep. The mapping of the outer edge to center deflection, however, cannot be exactly determined a priori, because processing variations in the silicon disc produce uncertainties in the thickness of the fulcrum and strength of the anodic bond. Therefore, the Zygo interferometer is used to calibrate the capacitance versus displacement function for each Nanogate.

To a first order approximation, the electrostatic coupling between the outer edge of the silicon diaphragm and gold trace on the Pyrex die can be modeled as a parallel plate capacitor, such that

$$C = \frac{\varepsilon_0 A}{d}, \quad (1)$$

where A is the area of the electrodes, d is the spacing of the electrodes, and ε_0 is the permittivity of free space. For small plate deflections, the capacitance varies as,

$$\Delta C = -\frac{\varepsilon_0 A}{d_0^2} \Delta d, \quad (2)$$

where d_0 is the initial undeflected distance and Δd is the displacement caused by the external deflection.

The initial separation of the outer edge of the silicon diaphragm is approximately 150μm with a total expected travel of 15μm. This means that the capacitance will vary up to 10% of the value at the undeflected state. The total area of the electrode pattern is approximately 24.5mm^2, resulting in an undeflected capacitance of approximately 1.45pF. With a target of better than 1 nm resolution at the center, it is necessary to measure capacitance with accuracy better than 0.3 femto farad or a signal-to-noise ratio of 74dB. The measurement resolution will be ultimately limited by noise and drift. By using synchronous detection as a measurement technique these parameters can be reduced.

It is important to note that the desired measurement accuracy (1nm) is obtainable even though the Zygo interferometer calibration is less accurate (2.4nm). This result is achieved by fitting the calibration data with a line regression, which has a sufficiently accurate gradient.
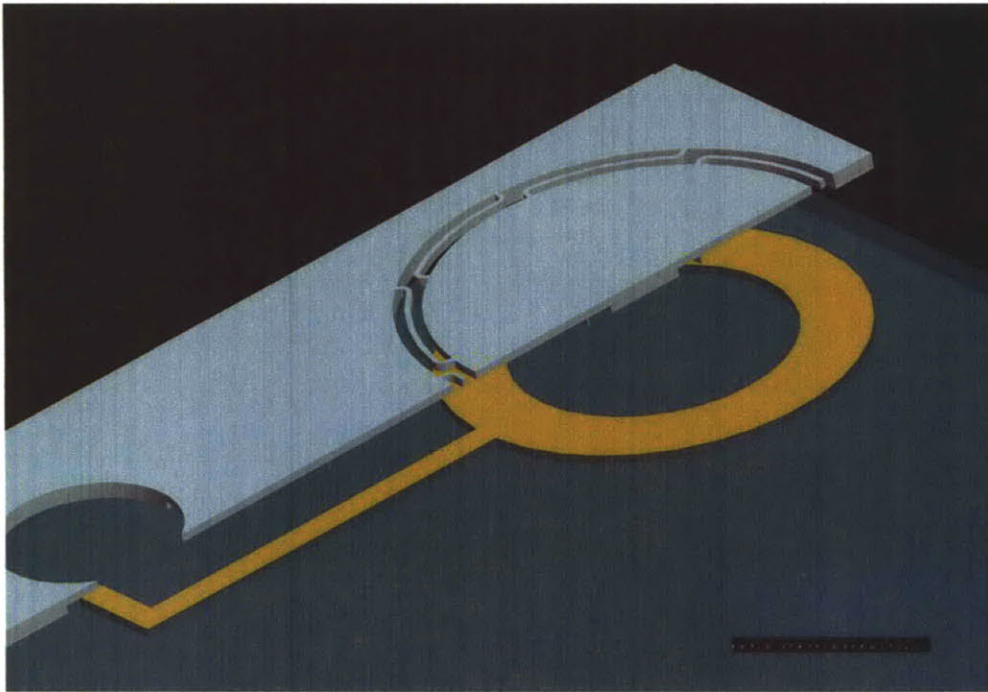
Figure 3: Cut-away diagram of the capacitive sensing electrodes. The silicon diaphragm is offset from the Pyrex diaphragm

3 Fabrication

This chapter describes the fabrication of the Nanogate from the design of the mask to a detailed description of the microfabrication process using the MEMS tools at Microsystems Technology Laboratory. The chapter concludes with a presentation of the fabrication results.

3.1 Mask Design and Fabrication Process Overview

The basic structure of the Nanogate, as described in Section 1.1, is a part of a larger silicon die designed to support electrical contact and fluid connections as shown in Figure 4, at the left. The main disc of the Nanogate occupies the top-left quadrant of the die. On the bottom side of the die (Figure 4, at the right), a rectangular trench runs from the disc area to one of the holes to house the capacitive electrode. The other two holes are designed as fluid inlet and outlet, and the window at the top-right quadrant is designed for observing fluid channels. Since the development of the capacitive measurement system does not require active fluid connections, these features are not used.
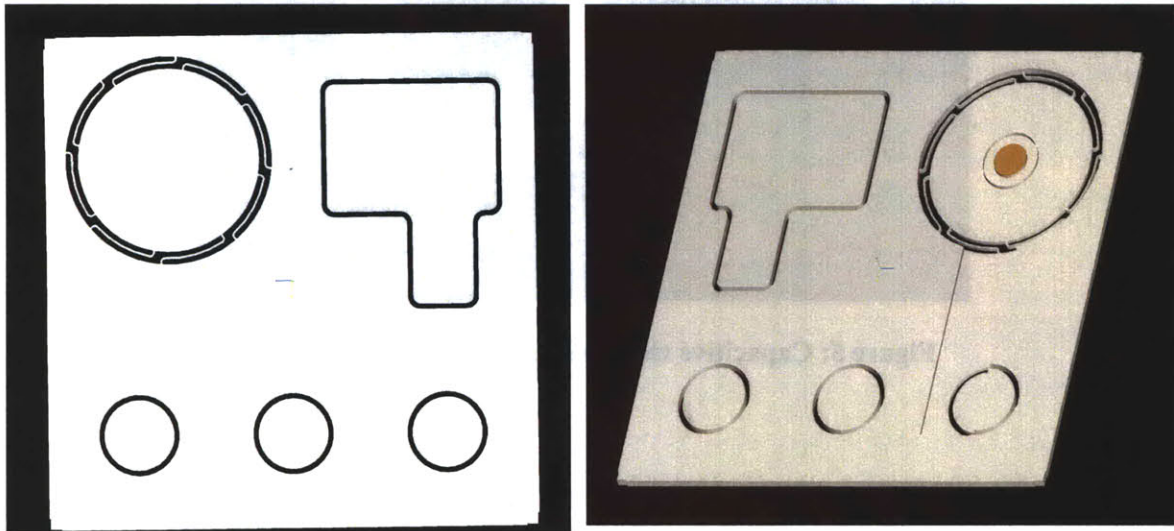
Figure 4: Nanogate die 3D model. Left: topview, Halo's are used to reduce etching time. Right: bottom view, a trench is designed to accommodate the capacitive electrodes on the Pyrex.

The Pyrex die is patterned with the capacitive electrode and aligns with the silicon die. As described in section 2.3, the electrode is a ring around the outside edge of the disc with an electrical contact inside the trench (Figure 3). In the future, when fluids are introduced into the Nanogate, the Pyrex die will be machined with additional features as microchannels and through-holes.

The silicon diaphragm and its corresponding Pyrex diaphragm are batch processed on wafers. Each wafer can hold a total of 14 dies with appropriate alignment and die-saw features. The silicon wafer is fabricated using two surface micromachining steps, one at the top surface and another at the bottom surface. One mask is required for each side. The masks are generated from a cross section of an assembly drawing of the dies. The larger through features are removed using halos to reduce the amount of etching necessary. A third mask is designed to pattern the Pyrex wafer with the electrode pattern in Figure 5.
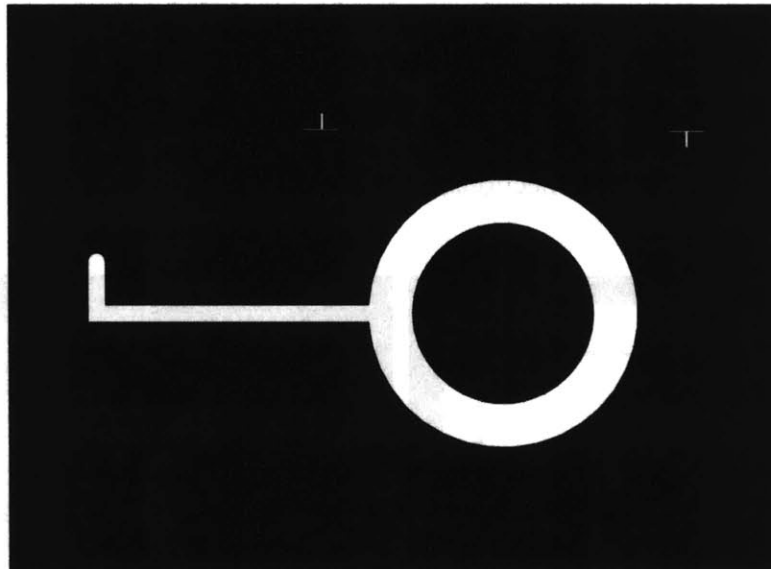
Figure 5: Capacitive electrode mask for the Pyrex wafer

3.2 Detailed Fabrication Process

This section outlines the detailed fabrication process for the Nanogate. Figure 6 shows an outline of the process flow.
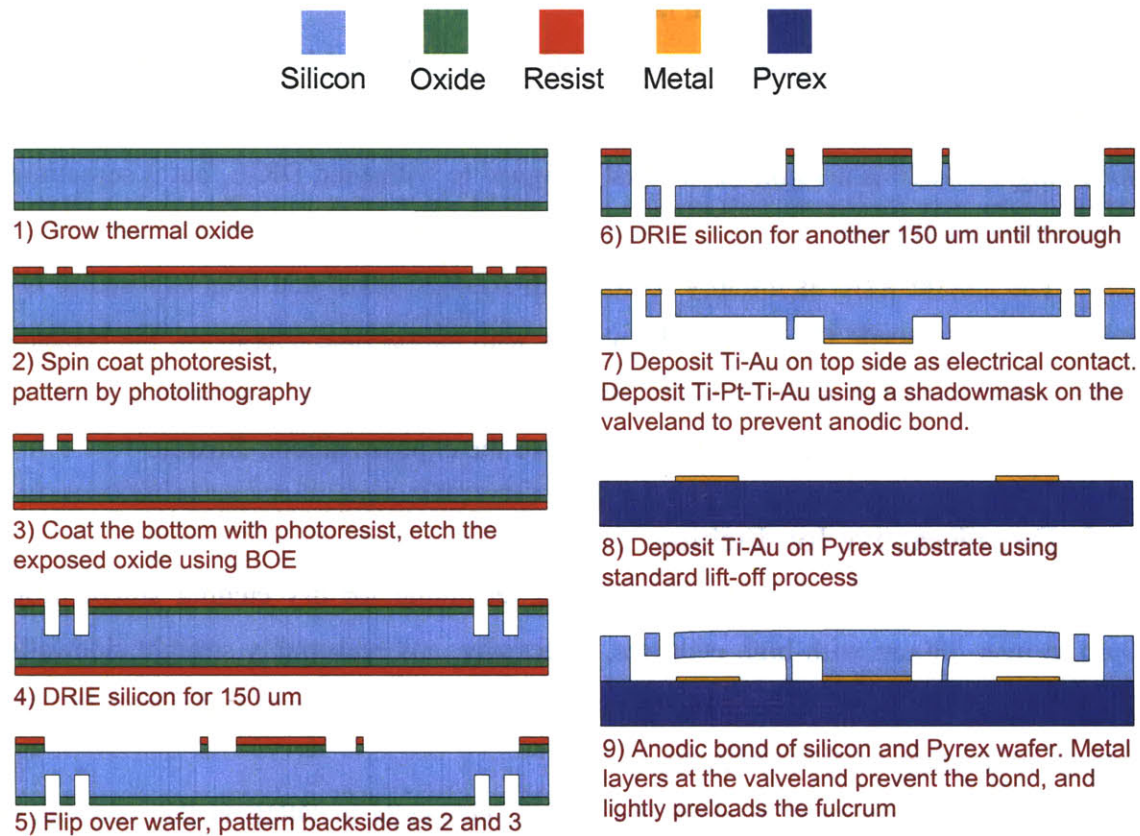
Figure 6: Outline of the Nanogate fabrication process, wafer shown in cross-section.

3.2.1 Materials and Preparation

The wafers used for this fabrication process are low resistivity (0.008 Ω-cm) n-type silicon wafers with specifications of 100mm in diameter, 300μm ($\pm$25μm) thick, and polished smooth on both sides. The preparations for photolithography involve cleaning the wafers using standard RCA clean and then thermally growing a 1μm silicon dioxide layer on the surface. The SiO_2 layer acts as a "hard mask" to preserve the pristine surface finish of the silicon wafer during the surface micromachining process. Previously, only photoresist had been used as a masking material and the micromachining process often contaminated the silicon surfaces and prevented proper anodic bonding.

3.2.2 Photolithography

The photolithography process for the Nanogate involves patterning a photoresist layer on the silicon wafer and then using buffered oxide etch (BOE) to make matching patterns in the silicon dioxide layer. The result is a silicon wafer masked with both silicon dioxide and photoresist as sacrificial layers.

There are two types of photoresist used in the lithographic process, OCG825 and AZ4620. OCG825 is a 1μm resist, which has great uniformity but cannot withstand DRIE processing. AZ4620 is a 10μm thick resist designed to withstand DRIE, but it sometimes leaves unwanted residue.

The silicon wafer is initially coated with AZ4620 resist and then exposed to UV using the topside mask. Developing the pattern with appropriate chemicals, the backside of the wafer is coated with OCG825 resist. With the front and backside masked by photoresist, the wafer is etched in BOE to remove the exposed silicon dioxide.

3.2.3 Deep Reactive Ion Etching

Deep reactive ion etching (DRIE) is a technique for dry etching silicon from 20μm to over 300μm with high etch rate, selectivity, and reasonably straight sidewalls. This technique has found widespread use in MEMS research because it is one of the few methods for through-wafer machining.

The key mechanism in obtaining straight sidewalls in DRIE is the passivation process which periodically coats the sidewalls with Teflon. However, incomplete removal of passivation gases can cause surface roughness and the undesired deposition of a material called "black silicon". It is therefore necessary to protect the surfaces of the silicon that are not to be etched with silicon dioxide.

The Nanogate wafers are etched using MTL's STS-2, commercial DRIE systems from Surface Technology Systems Ltd, Gwent, UK. Since the STS-2 uses a 6-inch wafer chuck, the prepared 4-inch silicon wafer is first mounted on a 6-inch handler wafer using the "target mount" method [21] developed by Dr. Ravi Khanna of the Microengine group at MTL. This technique can be used to adhere a 4-inch wafer to the 6-inch handler using AZ4620 resist to provide thermal contact to the wafer chuck.

The front side pattern is etched to a nominal depth of 150μm, but the actual etch depth is between 170 and 190μm to account for etch non-uniformities across the wafer. Non-uniformities can be reduced by rotating the wafer to several different orientations during the course of the recipe. The alignment marks are etched separately for a short duration and then covered with a small drop of AZ4620. After the desired depth has been reached, the wafer is first cleaned in oxygen plasma to remove any leftover Teflon. Then, it is Piranha cleaned to remove the photoresist and separate the Nanogate wafer from its handler.

3.2.4 Bottom Side Processing and Oxide Strip

After the desired patterns have been obtained on the top side of the Nanogate, a similar process is used to pattern the bottom side starting from the photolithography step. An additional alignment step is required to line up the front side patterns with the backside mask. The DRIE depth for the bottom side is approximately 150μm, with the etch completion gauged by the completion of the through features.

When features on both sides of the wafer have been completed, the silicon dioxide masking layer can be removed using 49% Hydrogen Fluoride (HF). Another Piranha clean is necessary following the oxide etch to make a thin layer of native oxide, which helps to keep the wafer clean after it is taken out of solution.

3.2.5 Metal Deposition

Both sides of the micromachined silicon wafer are deposited with metals using electron-beam deposition. The top side of the wafer is deposited with titanium and gold layers that act as electrical contacts to the silicon die. The gold layer is responsible for reducing the contact resistance caused by the native oxide on the silicon, while titanium layer is an adhesion layer for the gold.

On the bottom side, 4 layers of metal are deposited over the valveland designed to prevent anodic bond in the region (Figure 7). Starting from the bare silicon, the deposition sequence consists of titanium, platinum, titanium, and gold at thicknesses of 20nm, 100nm, 20nm, and 100nm. The gold layer, with no native oxide, is the primary deterrent of anodic bond. During the thermal cycles of the bonding process, however, the gold layer diffuses away from the silicon-glass interface and forms a eutectic with the

31

silicon, allowing anodic bonding to proceed. Therefore, a platinum layer is necessary to add a diffusion barrier between the gold and silicon layers. The titanium layers are included as adhesion layers between the silicon-platinum and platinum-gold interfaces.
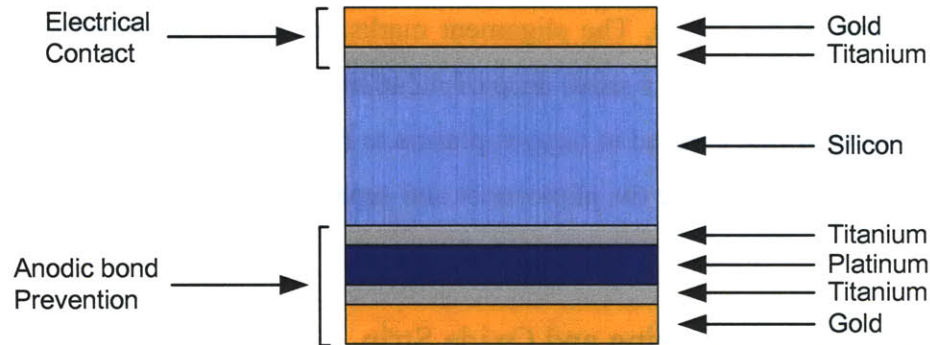
Figure 7: Metal Deposition on Silicon Wafer (not to scale)

3.2.6 Pyrex Wafer Processing

The wafers used to make the Pyrex substrate are 700µm thick, 100mm diameter Borofloat glass wafers from Mark Optics [22]. Processing on the Pyrex wafer involves photolithography and liftoff processes to deposit a pattern of metal traces that can be aligned with the silicon wafer. The Pyrex wafer is prepared using a Piranha clean and then coated with OCG825 photoresist. The wafer is then exposed with the electrode pattern shown in Figure 5 and developed. Similar to the silicon wafer, the Pyrex wafer is deposited with titanium as an adhesion layer and gold as the electrode. The final result is obtained by using acetone with ultrasound agitation to liftoff the metal deposited on top of the photoresist mask.

3.2.7 Anodic Bond and Diesaw

Anodic bonding is a process that joins silicon to Pyrex glass by applying a high voltage across the joint at the appropriate temperature and pressure. The positive electrode is connected to the silicon while the negative electrode is place to the Pyrex side. As the voltage is applied across the junction, Na+ ions in the Pyrex glass migrate away from the junction and O- ions migrate towards the junction. The O- ions oxidizes the silicon at the interface to form a strong covalent bond between the Pyrex and silicon.

The anodic bond between the Nanogate's silicon and Pyrex wafers are made at the wafer level using the EV501 aligner/bonder. Prior to the bonding process, the wafers

are rinsed in a sequence of acetone, methanol, isopropanol, and de-ionized water. Subsequently, the wafers are dried in the SRD spinner. Using the EV501 aligner, the wafers are carefully aligned and clamped together. The bonder recipe calls for 800V at 350°C and 1000 Newtons for approximately 30 minutes.

After the bond process has been completed, the excess sodium ions on the back of the Pyrex wafer are washed off using de-ionized water. Subsequently, the wafer is sliced into 20mm by 20mm dies according to the die-saw marks etched into the wafer.

In previous versions of this process, the anodic bond is made at die level after the silicon and Pyrex wafers had been diesawed individually. The resulting bond is often unreliable because of the particles introduced to the silicon and Pyrex surfaces by the diesawing process.

3.3   Fabrication Results

A few of the completed silicon-Pyrex dies have been deliberately broken to analyze the quality of the silicon and Pyrex surfaces at the valveland. The instruments used for this task are the scanning electron microscope (SEM) and the whitelight profilometer.

Figure 8 is a profilometer scan of the silicon surface measuring the roughness variations. It can be seen that less than 5nm peak-to-peak surface roughness has been preserved on the valveland surface. Figure 9 shows a SEM micrograph of the silicon diaphragm after the fulcrum has been deliberately is broken. When the silicon diaphragm is broken from the Pyrex diaphragm, almost a full ring of the fulcrum remained bonded to the Pyrex. This means the anodic bond is actually stronger than the fulcrum itself.
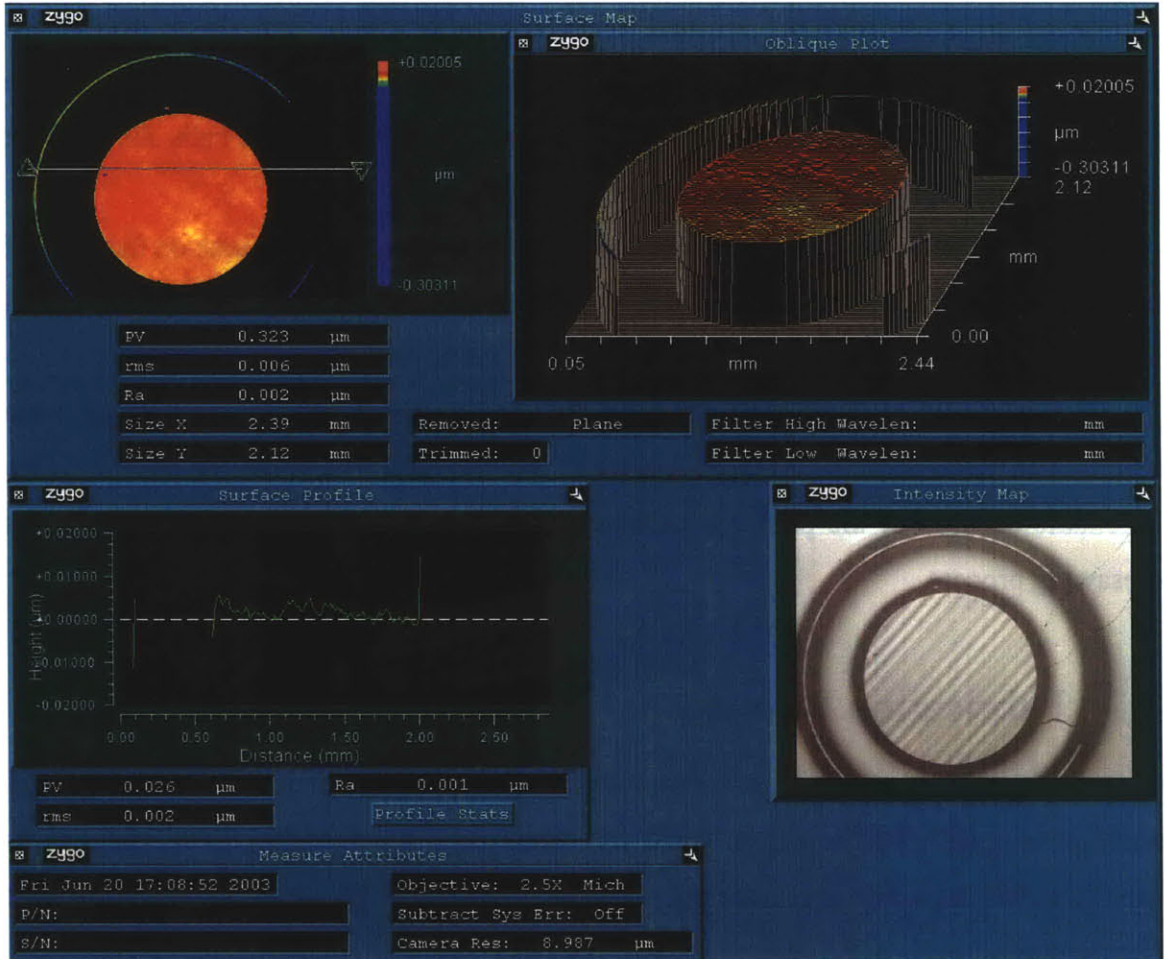
Figure 8: Profilometer scan of the silicon valveland showing 2nm rms surface roughness.

Figure 10 is a profilometer scan of the Pyrex surface after the silicon diaphragm is removed. The ring protrusion is an indentation made by the silicon valveland during the anodic bonding. The thermal cycle of the anodic bond brings the Pyrex wafer to a temperature where it reflows and conforms to the shape of the silicon diaphragm. This is an favorable result since the Pyrex wafer has inherently worse surface roughness than silicon, but the anodic bonding process can modify the Pyrex surface to produce mating silicon and Pyrex surfaces. Figure 11 shows a similar result as Figure 10 in a SEM micrograph.
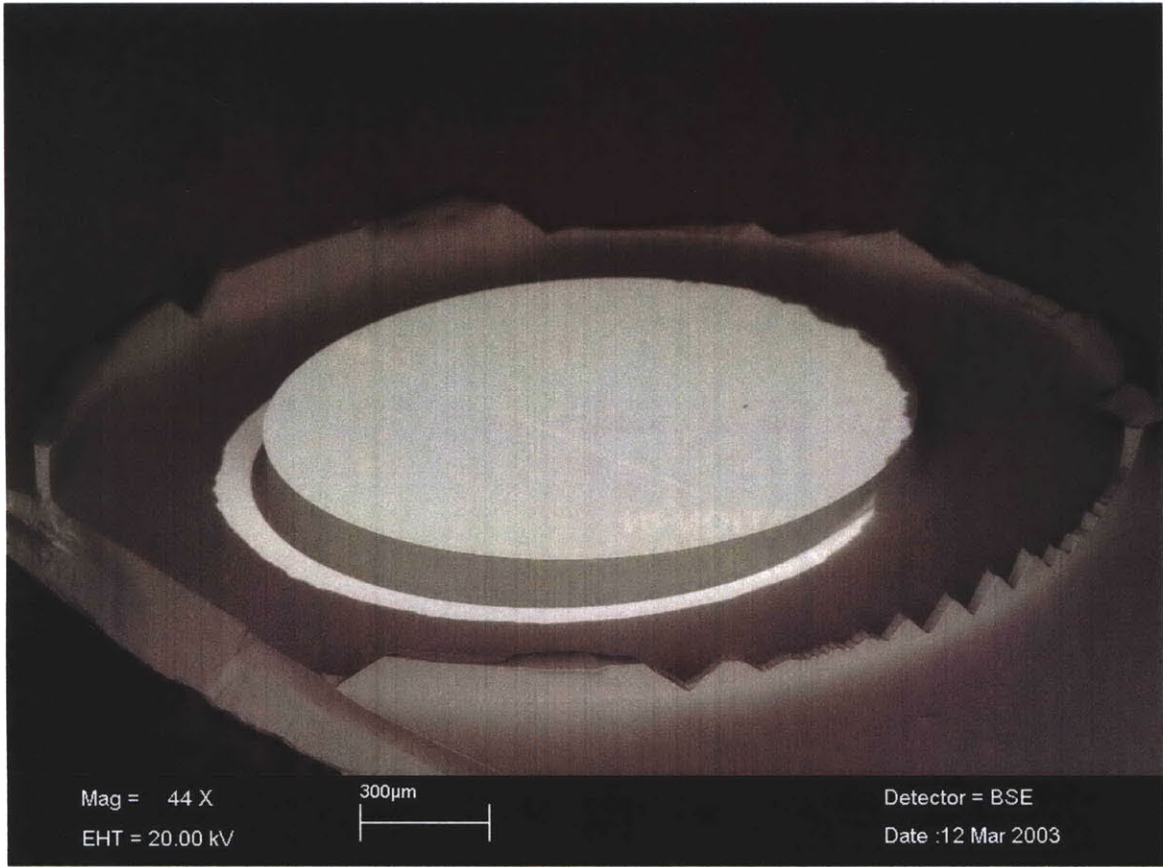
Figure 9: SEM Micrograph of the silicon diaphragm after the fulcrum is deliberately broken from the anodic bond with the Pyrex wafer
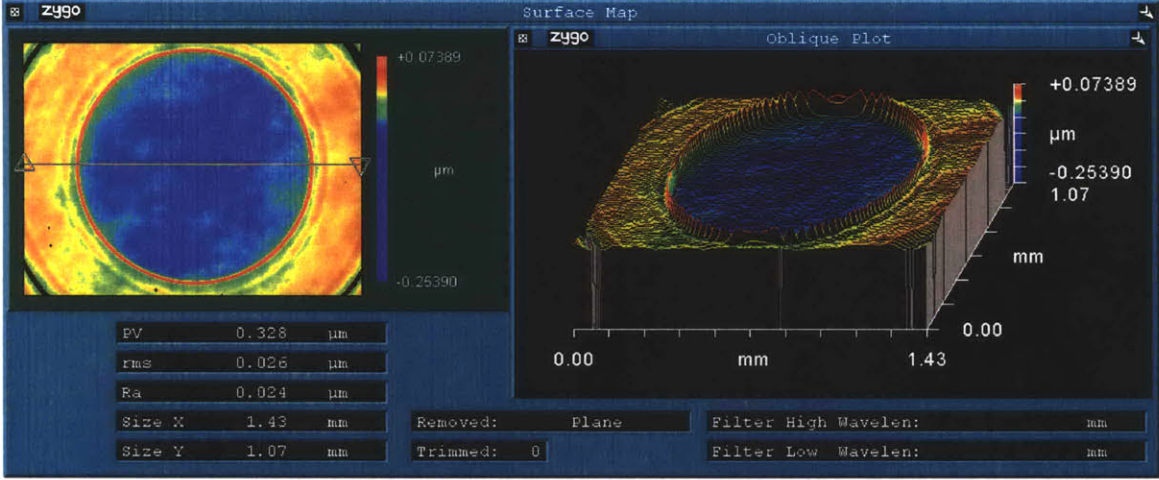
Figure 10: Profilometer scan of the Pyrex wafer after bonding. The reflow of the Pyrex wafer can be seen conforming to the shape of the silicon valveland. The remains of the fulcrum can be seen at the corners.

INDENTATION IN
PYREX SEAT

| Mag = 100 X | 200µm | Detector = BSE |
| EHT = 20.00 kV | | Date :12 Mar 2003 |
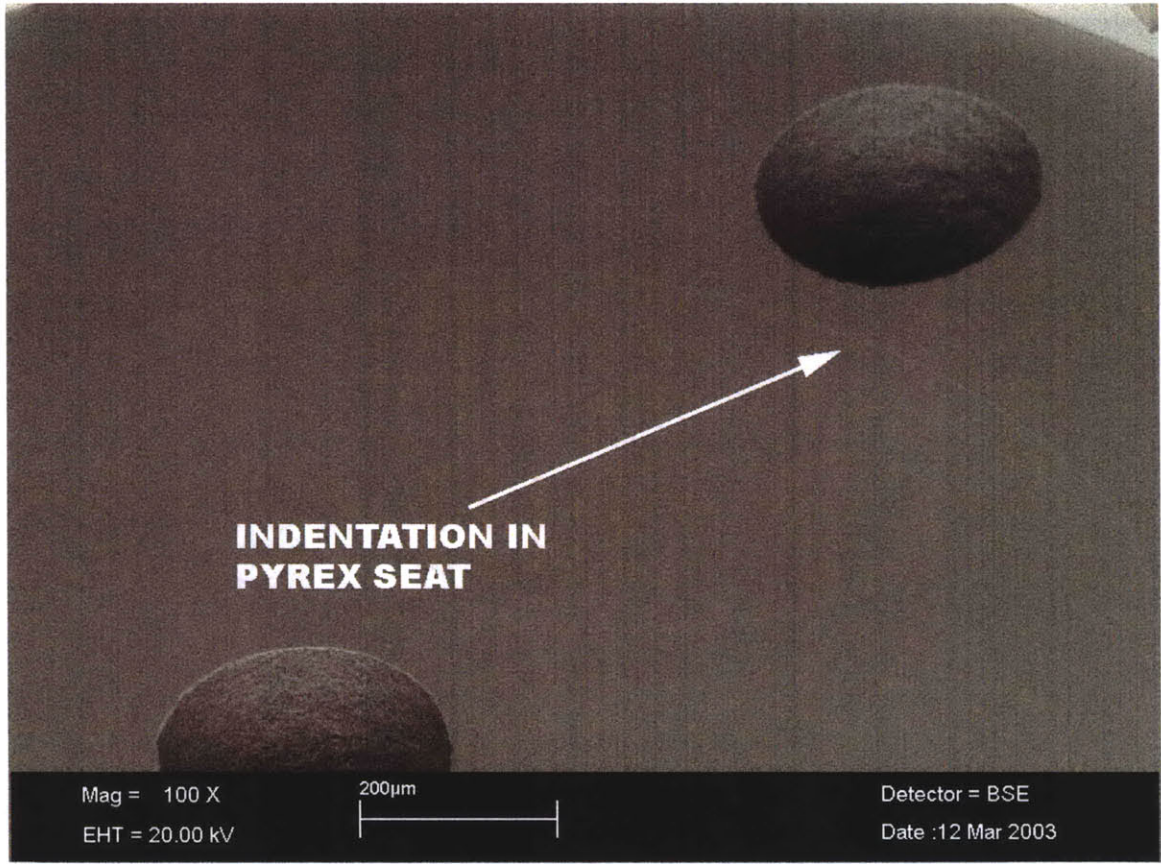
Figure 11: SEM of the Pyrex surface after bonding. The faint circle shows the indentation made by the silicon during the anodic bonding process.

4 Circuit Design

This chapter describes the electronic circuits associated with the capacitive measurement system's readout electronics. The analog front-end that converts capacitance to a voltage is described in Section 4.1, followed by the data acquisition system used to digitize the signal in Section 4.2. Finally, the physical implementations of these two subsystems are discussed in Section 4.3. Full schematics, printed circuit board layout, and accompanying software programs are included in the appendices.

4.1 Capacitive Sensing Front-end

The analog front-end converts capacitance to a voltage by exciting the Nanogate capacitor using an AC signal and using analog electronics to measure the electrical response to the signal. The circuitry for this task can be separated into three stages: an input amplifier to buffer the signal from the capacitor, a synchronous detector to mix the signal to DC, and an output filter to remove the out-of-band noise and to shift the output voltage to within range of the ADC (Figure 12) [18].
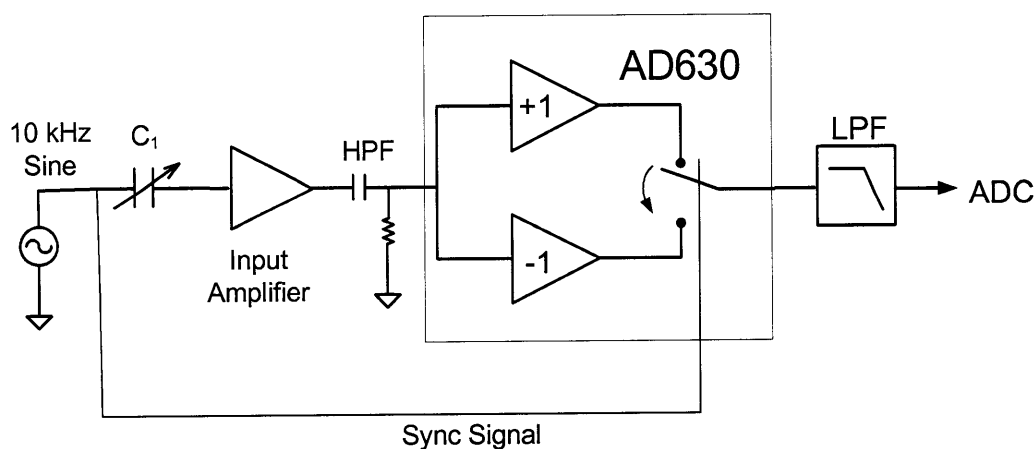
Figure 12: Capacitive sensing front-end

4.1.1 Input Amplifier

The purpose of the input amplifier is to measure the impedance of the Nanogate capacitor C_1 with the least amount of signal degradation caused by parasitic capacitance,

parasitic resistance, and noise. Parasitic capacitance attenuates the response to the measured capacitance and is mainly found between the capacitive sensing electrode and the printed circuit board (PCB), as well as between the input pin and other pins of the amplifier. Modeled as parallel to the capacitor of interest, the parasitic capacitance reduces the measured signal and may vary with time, temperature, and humidity. Parasitic capacitance can be minimized by using guard electrodes around the input that are bootstrapped to the input voltage (dotted lines in Figure 13). Parasitic resistance refers to the leakage current through the input of the amplifier. Its effects on the signal are similar to those of parasitic capacitance. In addition to the use of guard electrodes, parasitic resistance can be minimized by thoroughly cleaning the PCB using flux remover and by choosing amplifiers that are specifically designed for low input bias current.

High Impedance
Non-Inverting Configuration

Low Impedance
Inverting Configuration
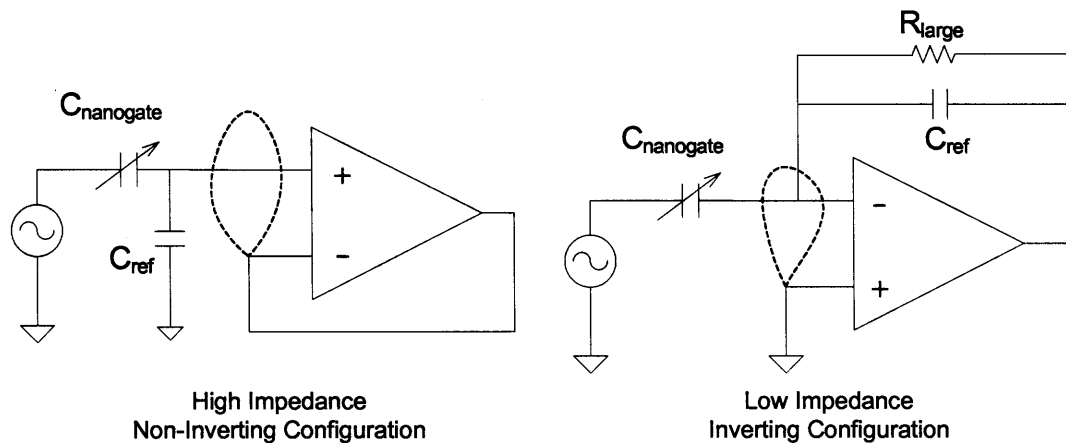
Figure 13: Input amplifier in high and low impedance configuration

There are two fundamental circuit topologies for detecting signal from a capacitive sensor: using a high impedance input to measure voltage and using a low impedance input to measure current (Figure 13). In the high impedance (non-inverting) case, the Nanogate capacitor is a part of a capacitive divider, and the input of the amplifier moves with the voltage of the signal. In the low impedance (inverting) case, the input of the amplifier is at a virtual ground and a reference capacitor is used in feedback; the capacitively coupled current is converted into a voltage by a transimpedance amplifier. The low impedance configuration is chosen over the high impedance configuration because the full excitation signal can be applied to the Nanogate capacitor compared to only half in the high impedance configuration. Additionally, since the input

38

of the amplifier is a virtual ground in the low impedance configuration, the operating point of the amplifier is constant, and therefore less prone to common-mode errors.

The OPA129 [23] operational amplifier is chosen as the input amplifier because it offers extremely low input bias current of 100fA maximum. Its minimum unity-gain bandwidth is 0.7MHz, which provides a loop gain of 70 at 10kHz excitation. The input-referred noise at 10kHz is specified at $15nV/(Hz)^{-\frac{1}{2}}$ voltage noise and $0.1fA/(Hz)^{-\frac{1}{2}}$ current noise.

The input amplifier circuit is shown in Figure 14. C_1 is the Nanogate capacitor, and C_2 is a reference capacitor of approximately the same value as C_1. R_1, R_2, and R_3 form a resistive T-network to provide a high impedance DC path to ensure that the inverting input does not float to arbitrary voltages.

$$\frac{V_{out}}{V_{in}} = \frac{C_1}{C_2}, \quad \text{if } f_{excitation} \gg \frac{1}{2\pi R_{fb}C}, (3)$$

where R_{fb} is the equivalent parallel resistance to C_2. The T-network formed by R_1, R_2, and R_3 reduces the feedback to the input by the ratio of R_2/R_3 and, consequently, magnifies the effective parallel resistance to C_2 by the same factor. An effective parallel resistance of 500MΩ is achievable, far beyond the value that can be realized using conventional components. The resulting time constant of the feedback loop is approximately 100Hz, which satisfies the condition of equation 3 for a $f_{excitation}$ of 10kHz.

The disadvantage of the T-network is that the offset of the input amplifier is also multiplied by the same ratio as the feedback resistance. Therefore, output of the input amplifier is AC coupled to the next stage to eliminate errors caused by offset drift.
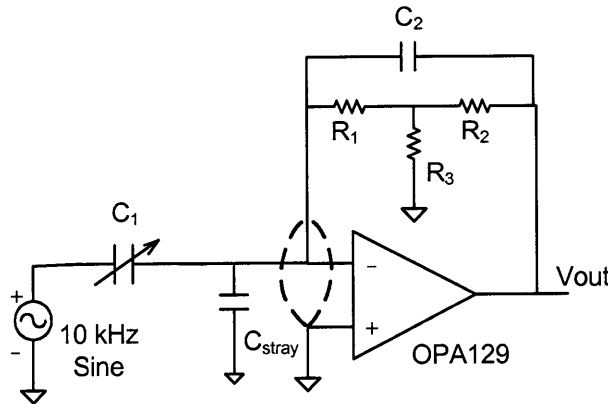
Figure 14: Input Amplifier Schematic

4.1.2 Synchronous Detector

Synchronous detection is a signal conditioning technique designed to detect the amplitude of a fixed-frequency signal in the presence of noise. In this scheme the measured signal is multiplied with a reference signal of the same frequency and phase. The amplitude of the desired signal is therefore transformed down to DC, while low frequency noise is transformed up to the reference frequency. The output of the multiplier can then be low-pass filtered to remove the noise at the reference frequency and beyond.

The multiplier that follows the input amplifier is the AD630 precision modulator from Analog Devices [24]. The AD630 has two parallel amplifiers with gains of +1 and -1, and switches the output between the two amplifiers at the frequency of the reference signal. This has the effect of multiplying the input signal with a square wave at the reference frequency, and it is insensitive to amplitude of the reference signal. Figure 12 shows the simplified schematic of the AD630 where the input signal is the output of the OPA129 and the reference signal comes from a TTL gate derived from the 10kHz sinusoidal source.

4.1.3 Output Signal Conditioning

The output of the AD630 is level shifted and low-pass filtered before being digitized by an ADC. The level shift moves the DC level of the output to a voltage range acceptable for the ADC, and is implemented using a LT1007 operational amplifier [25] in an inverting configuration with unity gain (Figure 15). The amount of shift is determined by the voltage at the non-inverting terminal, which is set by a LT1019 bandgap reference [26] followed by a voltage divider.

The low-pass filter removes out-of-band signals from synchronous detection and sets the total system bandwidth. A four-pole voltage-controlled voltage-source (VCVS) filter is implemented using two LT1007 operational amplifiers (Figure 15) [27, 28]. This filter has a bandwidth of 160 Hz and a total gain of 2.5.
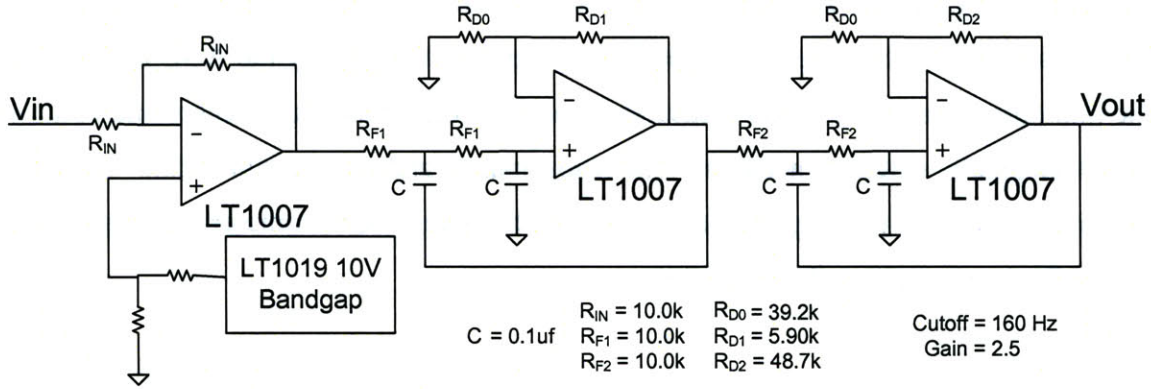
Figure 15: Level shifter and 4-pole VCVS low-pass filter

4.1.4 Switched Calibration

The long-term variation in the offset of the AD630 and the output stage is calibrated using a switched reference source at the input of the AD630 (Figure 16). At periodic instances a reference signal is switched into the AD630 and its result is stored and used as the overall system offset. The reference signal is generated using an identical OPA129 input amplifier where the Nanogate has been replaced by a reference capacitor. The switch is implemented using an AD451, a low on-resistance analog switch.
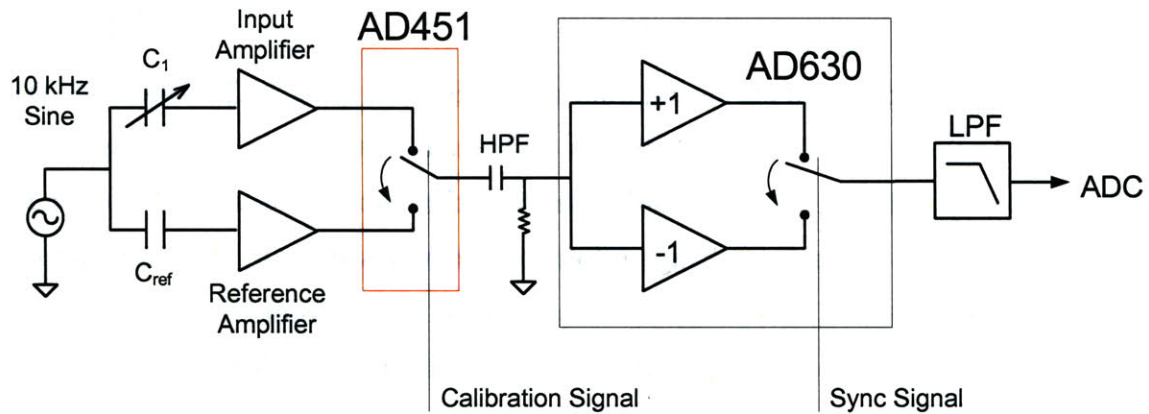
Figure 16: Switched calibration circuit

4.2   Data Acquisition System

A custom data acquisition system is designed to digitize the output of the analog section. The three main components of this system include a high resolution ADC, a

microprocessor, and a computer. A temperature sensor is also included to measure signal drift as a function of temperature. The analog input is digitized by the ADC and read by the microprocessor, which also measures input from the temperature sensor and controls the Nanogate's external actuator. The capacitance and temperature data from the microprocessor and the displacement data from the Zygo interferometer are logged by a Visual Basic program on the computer.
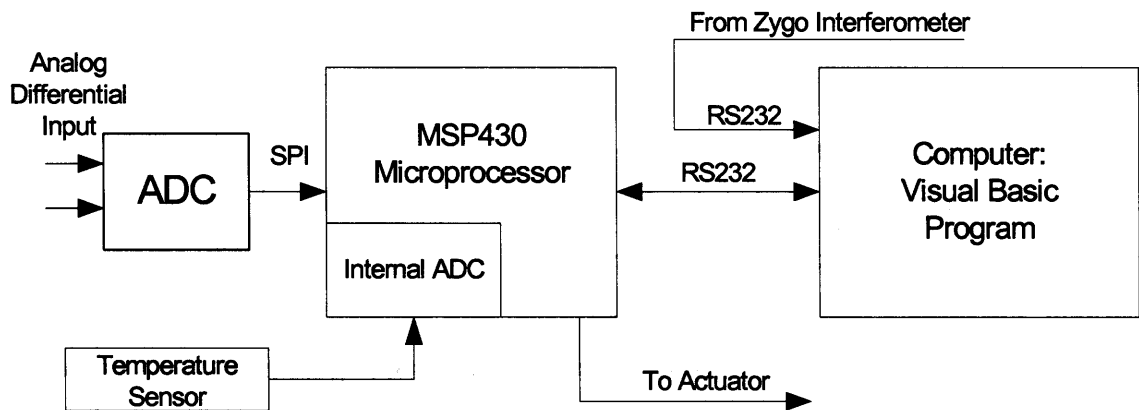
Figure 17: Data Acquisition System

4.2.1 Analog to Digital Conversion

Voltage output from the analog front-end is digitized using a LTC2440 ADC from Linear Technology [29]. The LTC2440 is a differential input with a 2.5V range and 24 bits digital output. The maximum sampling rate is 4 kilo-samples-per-second (ksps) but is settable to allow the user to exchange resolution for bandwidth. On this particular data acquisition board, the LTC2440 is set to sample at 1 ksps, which corresponds to an effective resolution of 114 dB, significantly more than the required 74 dB.

4.2.2 MSP430 Microprocessor

The functions of the microprocessor include reading data from the ADC, measuring temperature, controlling the Nanogate's external actuator, and relaying data to the computer. The MSP430 microprocessor series from Texas Instruments is chosen because of its programmability. Specifically, the MSP430F149 [30] is used. It has 60 kilobytes of flash program memory, an internal 12-bit ADC, 2 timers, and can be clocked

up to 8MHz. The microprocessor communicates with the ADC over a 3-wire SPI interface.

The temperature is measured using an AD592 temperature dependent current source [31]. The AD592 sources current proportional to absolute temperature at a ratio of 1 uA/K. The output current is converted to voltage via a resistor and digitized using the MSP430's 12-bit internal ADC. The measured temperature resolution is 0.125°C.

The Nanogate actuator is controlled via several digital lines provided by the MSP430. These signals include clock, step command, and direction. Since the actuator takes in 5V TTL signals and the MSP430 runs at 3.3V, a Schmidt-triggered inverter is used as an interface.

The MSP430 communicates with the computer via a serial line at 57.6 kbits/s. The internal UART of the MSP430 is connected to a RS-232 line driver, which is connected to a computer using a standard 9-pin serial connector.

4.2.3 Visual Basic Data Logger and User Interface

Capacitance, temperature, and displacement from the Zygo interferometer are read by a Visual Basic program (Figure 18), which stores the data on disk and provides a real-time stripchart display. This program is also allows the user to send commands to control the external actuator via the microprocessor. The actuator motion can be controlled by single commands or a script that automatically performs motion (up, down, and wait) sequences.
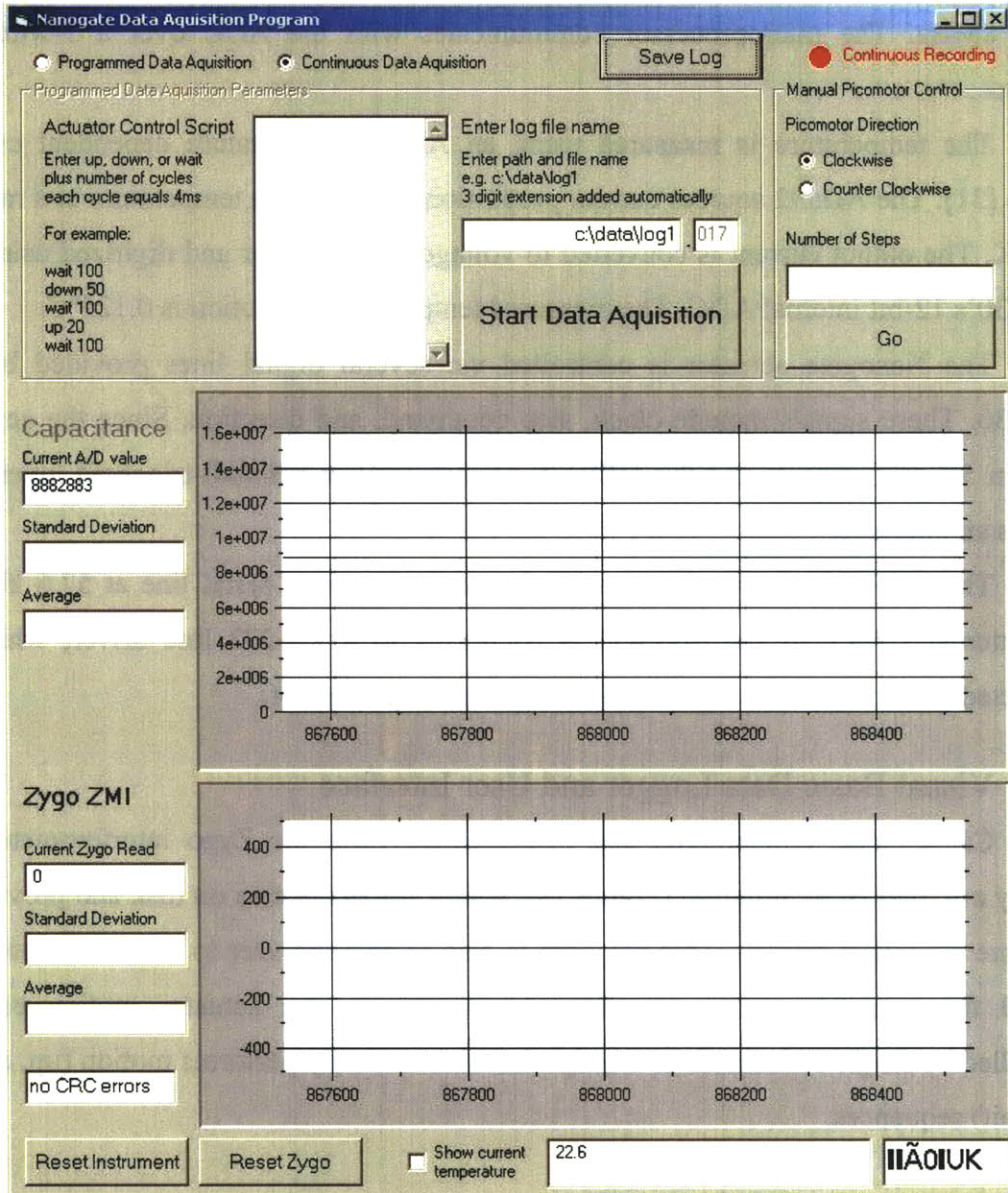
Figure 18: Screen-shot of the Visual Basic data collection and user interface program

4.3 Physical Circuit Considerations

4.3.1 Electrical Contact to Capacitive Electrodes

The capacitive electrodes on the silicon and Pyrex part of Nanogate are connected to the analog front-end via thin, flexible copper wires (Figure 19). The wires are bonded by conductive epoxy [32] to the electrodes on the Nanogate and are soldered to pads on the printed circuit board. The wires are single strands taken from standard 26 gauge stranded wire.
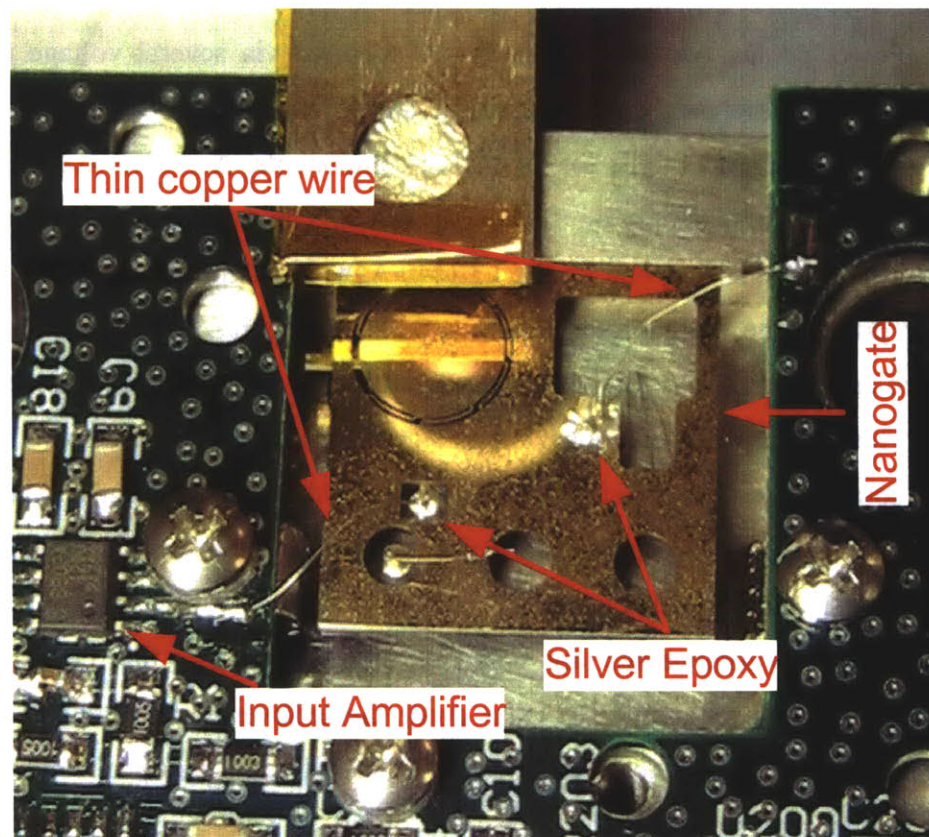
Figure 19: Electrical connection between capacitive electrodes and input amplifier

4.3.2 Printed Circuit Board Design and Layout

The analog front-end and data acquisition circuits are implemented on standard 2-layer, 62 mil, FR-4 printed circuit boards (PCB). The two circuits are made on separate boards in order to minimize interference between the two circuits and to modularize the development effort. The signal lines between the two PCBs are connected via SMA-type

coaxial cable, which provide a shielded electrical connection with a flexible mechanical connection.

Ground planes are used extensively on the two PCBs to reduce the interference caused by external electromagnetic fields. All components are placed on the top of the circuit board so that a complete ground plane can be formed on the bottom side of the PCB. The data acquisition PCB has separate ground planes between the ADC and the microprocessor section of the board in order to reduce the effect of digital noise on the ADC. The two PCBs are also enclosed in a grounded metal box for shielding against external interference signals.

Power on the two circuit boards are supplied via several voltage regulators to minimize the interference coupled through the power supply. The analog front-end is supplied +12V and -12V rails for its analog components. A dedicated 5V digital rail is provided for the logic supply on the analog switch. The data acquisition circuit board is powered with a 5V analog line for the LT2440 ADC and temperature sensor, a 5V digital line for driving the picomotor actuator, a 3.3V analog rail for the ADC onboard the microprocessor, and a 3.3V digital rail for digital functions on the microprocessor.

The placement of components and signal lines on the circuit board is also given careful consideration. Every effort is made to keep the length of signal lines as short as possible and components that can add noise to the signal line, such as digital logic gates, are deliberately placed farther away.

After the components are soldered onto the board, the PCBs are cleaned extensively with flux-remover to clear away the leftover flux residue. Since the DC impedances on the circuit board range from 10-500 MΩ, the electrical conduction of flux can be a significant parasitic.

Figure 20 and Figure 21 are photographs of the analog front-end and data acquisition PCBs. The detailed schematic and PCB layout are shown in Appendix C.
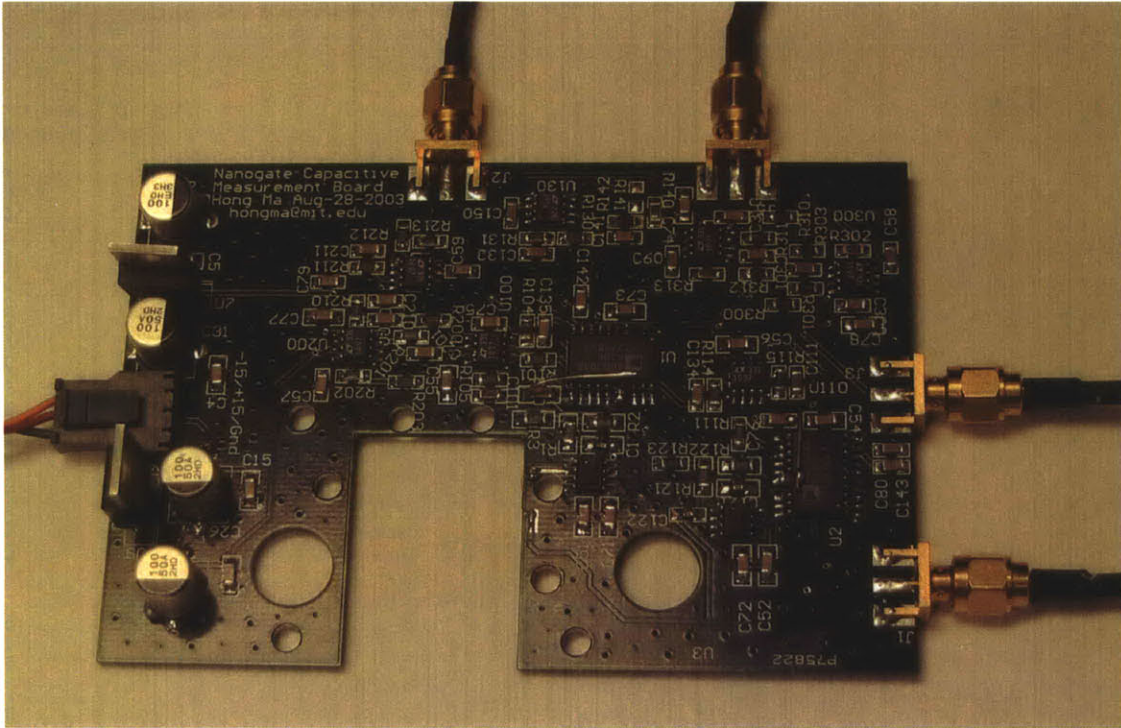
Figure 20: Photograph of the analog front-end PCB
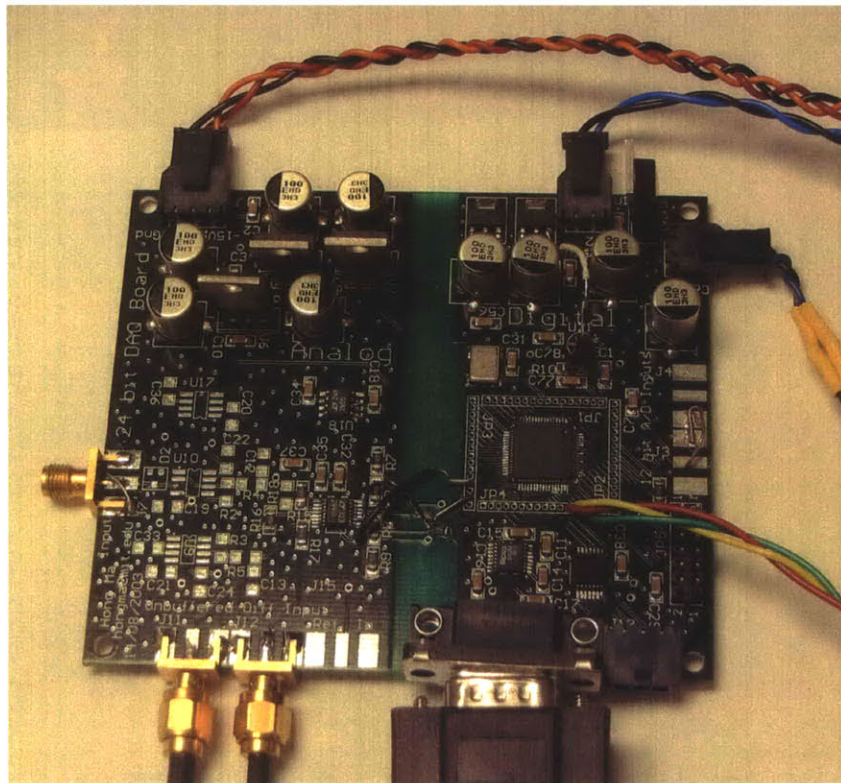
Figure 21: Photograph of the data acquisition PCB showing split ground planes for the ADC (left side) and microprocessor (right side)

5 Results and Discussion

This chapter presents the results from testing the capacitive displacement sensor. Section 5.1 describes the results of the capacitance versus displacement measurement. Section 5.2 analyzes the noise floor of the capacitance measurement. Finally, section 5.3 examines the drift error of the capacitance measurement.

5.1 Capacitance versus Displacement

As discussed in section 2.3, each Nanogate device needs to be calibrated using the Zygo interferometer. As external deflection is applied to the silicon diaphragm, the data acquisition software records the value of the ADC from the capacitive measurement circuit, displacement as measured by the Zygo interferometer, and the room temperature. In order to minimize drift in the Zygo readings caused by air currents, the laser beam is shielded using acrylic tubes. Figure 22 shows the sequence of actuator deflections, Figure 23 shows the response of the capacitive sensor, and Figure 24 shows the response of the Zygo interferometer. The droop of the capacitance and Zygo output after each set of input steps is an artifact of the actuator assembly: The force on the silicon diaphragm is applied through an o-ring, which has a relatively slow relaxation time.

Figure 25 shows the calibration of Zygo measured displacement versus capacitance. This graph has three distinct regions. In region I, the capacitance is increasing in response to the deflection from the actuator while the central valveland remains fixed. This is because the deflection of the outer edge must first overcome the preload due to the additional thickness of the metal film layer that causes the diaphragm to bend during the anodic bonding. Region III shows the valveland displacement varying as a linear function of capacitance as in equation (2). Region II is the non-linear, transition between regions I and III. It is hypothesized that this transition region is caused by asymmetry in the actuation of the outer edge of the silicon diaphragm and with better actuation schemes the rounded region can be reduced. The roundedness of this region makes it difficult to define a zero point. It is possible to interpolate this point by fitting a straight line to region III in Figure 25 and finding its intercept with the mean of region I.

Figure 26 shows the Zygo versus capacitance plot subtracted from its linear fit line in region III of Figure 25. A periodic fine structure, on the order of 5nm, is revealed and consistent during both the opening and the closing of the Nanogate. The source of this behavior is likely an artifact of the actuator and how it interacts with the mounting structure, however, more analysis is necessary to fully understand this problem.
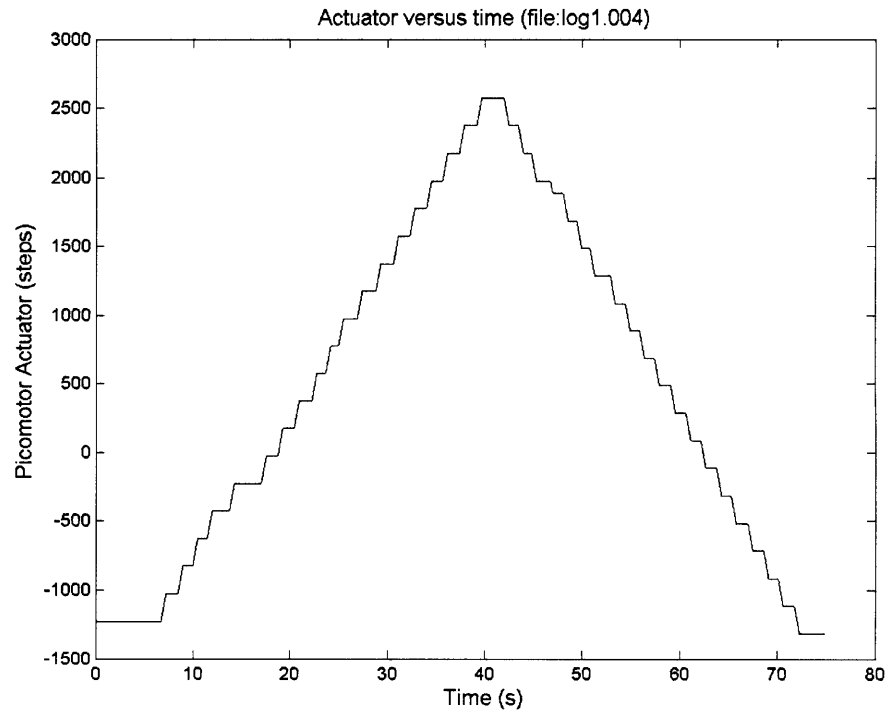

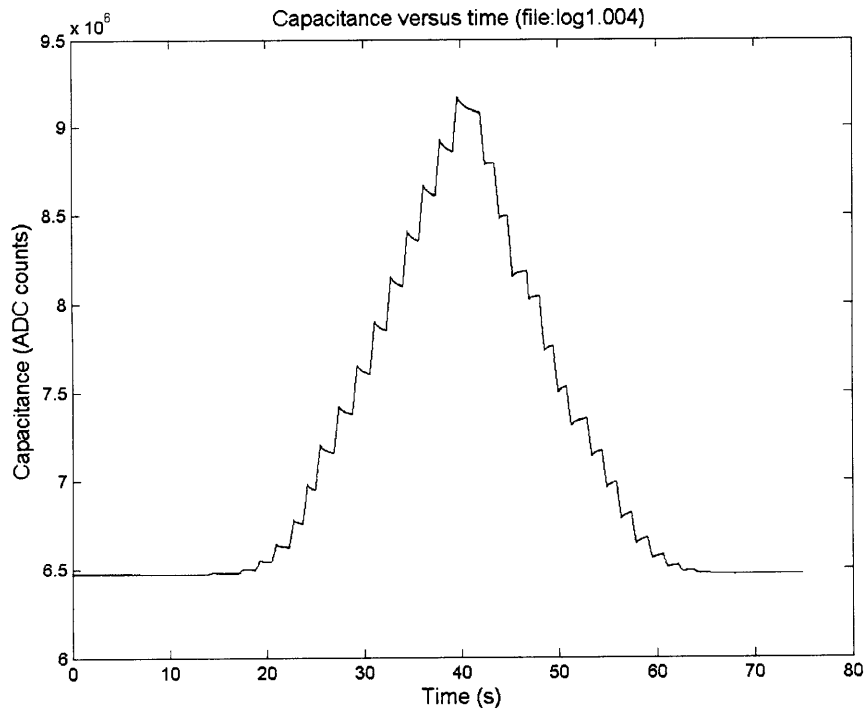**Figure 22: Actuator command versus time**

Figure 23: Capacitance output in ADC counts versus time
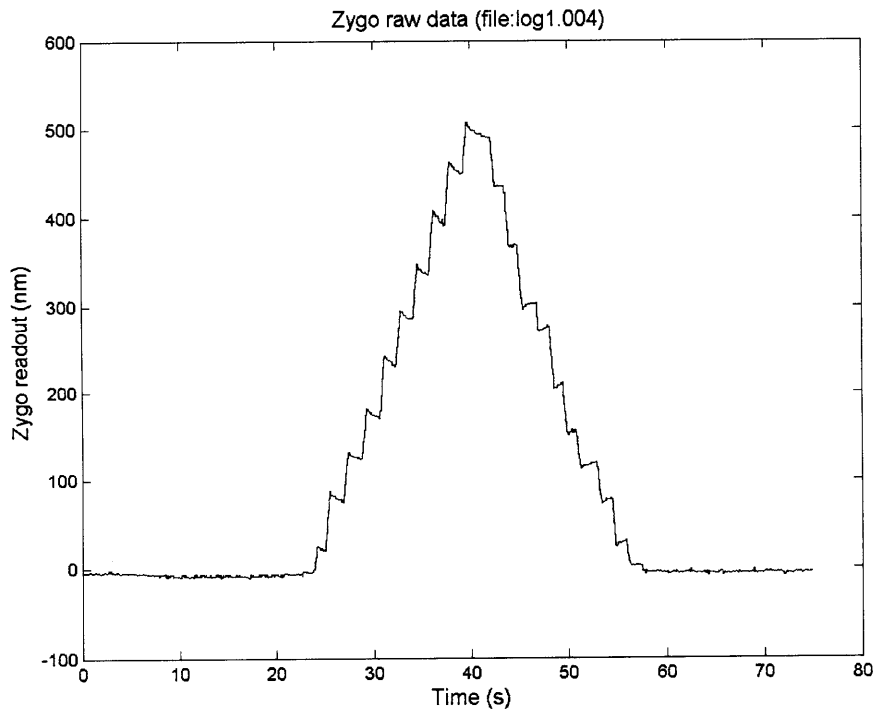
Figure 24: Zygo output versus time
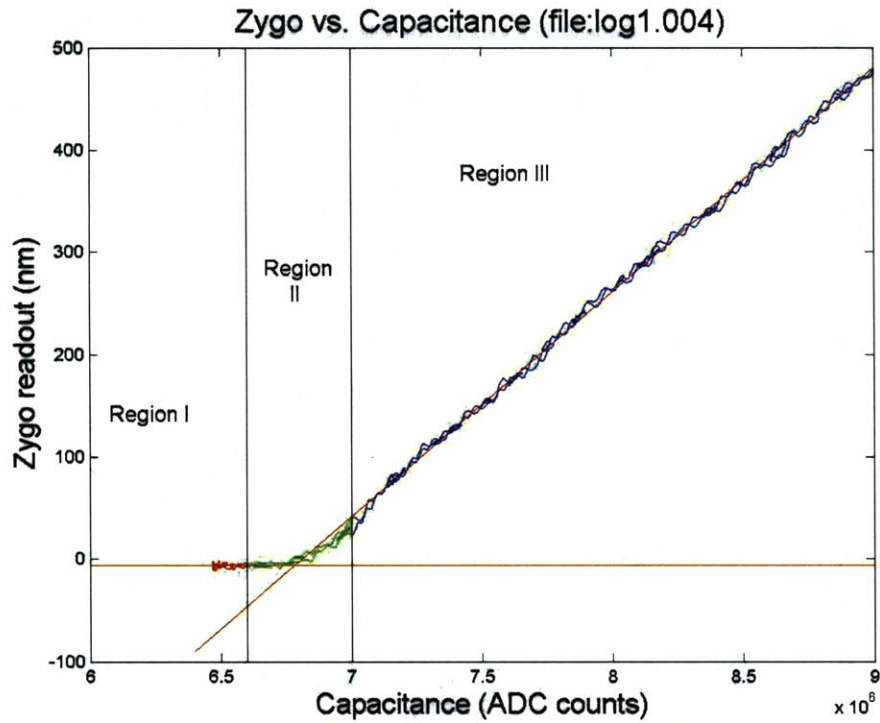
Figure 25: Zygo vs. Capacitance divided into 3 regions
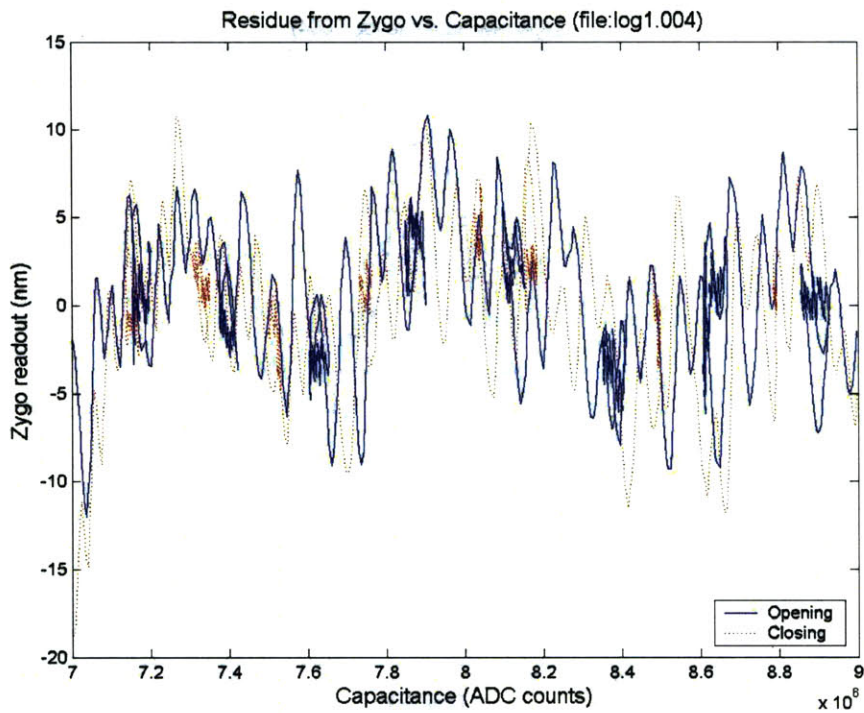
Figure 26: Residue plot of Zygo vs. Capacitance minus its linear fit line in region III of Figure 25

5.2 Noise Analysis

Noise is inherent to all electronic systems and fundamentally limits measurement resolution. Noise can be classified by its spectral response as stray pickup, white noise, and 1/f noise. 1/f noise is considered as part of drift and will be discussed in the next section.

Stray pickup is the coupling of interference signals from sources near the circuit such as microprocessors, CRTs, and power lines. In the design of the capacitive sensor, stray pickup is minimized by careful layout of the printed circuit board. These considerations include surrounding all signal lines with ground planes, using separate power supplies and ground planes for analog and digital circuits, and shielding the entire circuit in a grounded metal box. Since stray pickup cannot be easily predicted, it is measured experimentally along with white noise.

White noise has a flat spectral density and its integral over the total system bandwidth represents the output amplitude. In passive dissipative elements, namely resistors, the source for white noise is attributed to Johnson or thermal noise; in active elements, the source for white noise is attributed to shot noise. White noise is minimized by the choice of appropriate passive and active devices. In the capacitive sensing analog front-end circuit, white noise can be calculated by summing the specified noise power of each device and integrating it over the total bandwidth, which is set by the bandwidth of the output filter at 160Hz.

The circuit elements that contribute to white noise are the OPA129 input amplifier, AD630, LT1019 bandgap reference, and the three LT1007 amplifiers that make up the level shifter and output filter. The noise from the bandgap reference, level-shifter and output amplifier can be measured separately by disconnecting the input from the AD630. Figure 27 shows a noise waveform measured using the LTC2440 ADC, where the RMS variation is 5.6µV and a peak-to-peak variation of approximately 30µV

The noise band of interest for the OPA129 and AD630 is centered at 10 kHz with a bandwidth of 320 Hz. The bandwidth is doubled due to the frequency conversion in the synchronous detection process. The measured noise of the entire analog front-end is shown in Figure 28, where the RMS variation of 37µV or equivalently 0.056nm, and a peak-to-peak variation of 200µV or 0.3nm. Practically, the expected resolution can be

taken as an average of the RMS and peak-to-peak value at 0.2nm. As a matter of reference this is equivalent to 0.1 femto farad of capacitive change.
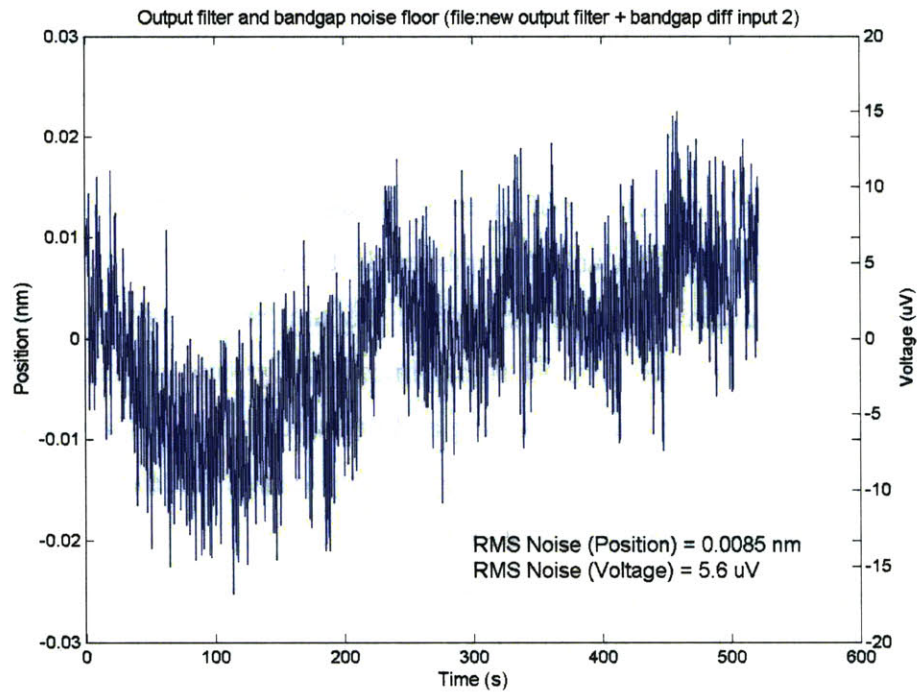
Figure 27: Noise waveform from the output filter and bandgap reference
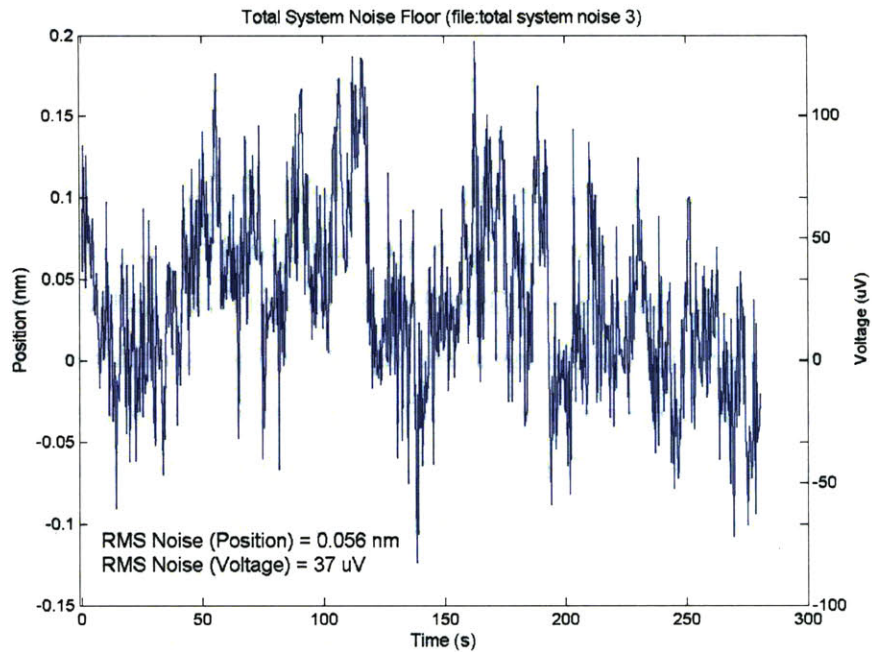
Figure 28: Noise waveform of the full differential capacitive sensing circuit

5.3 Drift Analysis

Drift is the variation in system output over long periods of time and is caused by variations on circuit parameters such as resistance, amplifier offset, and circuit gain. The causes of these variations include temperature, humidity, and slow relaxation processes in the circuit elements and on the circuit board. The function blocks that affect output drift are the bandgap reference, the output filter, the AD630, and input amplifier.

Figure 29 and Figure 30 shows the output drift and temperature dependence from only the bandgap reference and the output filter. The results are stable to within 0.05nm, smaller the noise floor of the analog front-end circuit. Shown in Figure 31 and Figure 32, drift from AD630 is significantly higher and temperature dependent. Using the calibration scheme discussed in Section 4.1.4, this drift can be compensated to within 1nm of variation (Figure 34) in a span of 20 hours. Figure 34 shows drift at the output in the presence a lot of external disturbances due to activity in the lab. The calibration is able to compensate most of the variation, but the peak-to-peak variation due to drift is now 2nm. This result shows that in order to minimize drift, careful consideration must be give to shielding and environmental control around the measurement system.

Offset variation in the OPA129 does not cause drift at the output because the signal from the OPA129 is AC coupled into the AD630. However, variation in gain between the input and reference amplifiers also causes output drift and cannot be corrected under the current calibration scheme. One way to solve this problem is to switch in a reference capacitor in parallel with the Nanogate. This scheme presents additional difficulties as settling time for the switching transients may become an issue.

It is important to note that the gain of the input and reference amplifiers operate under extremely high impedance and is sensitive to parasitic conduction on the PCB and therefore, the cleanliness of the PCB. In future monolithic implementations where the entire circuit can be enclose in a hermetically sealed package, this issue may be drastically improved.
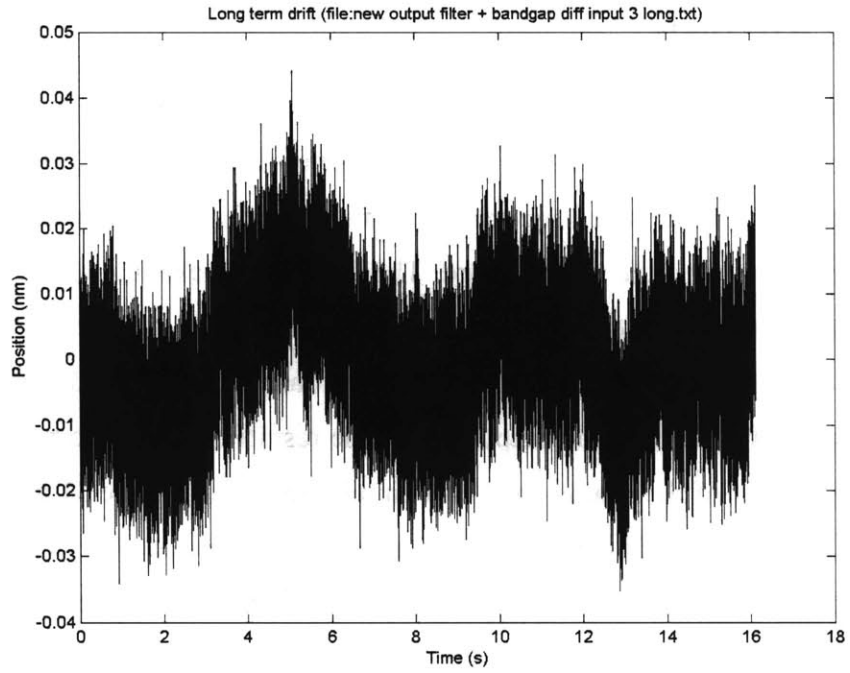
Figure 29: Drift from bandgap reference and output filter
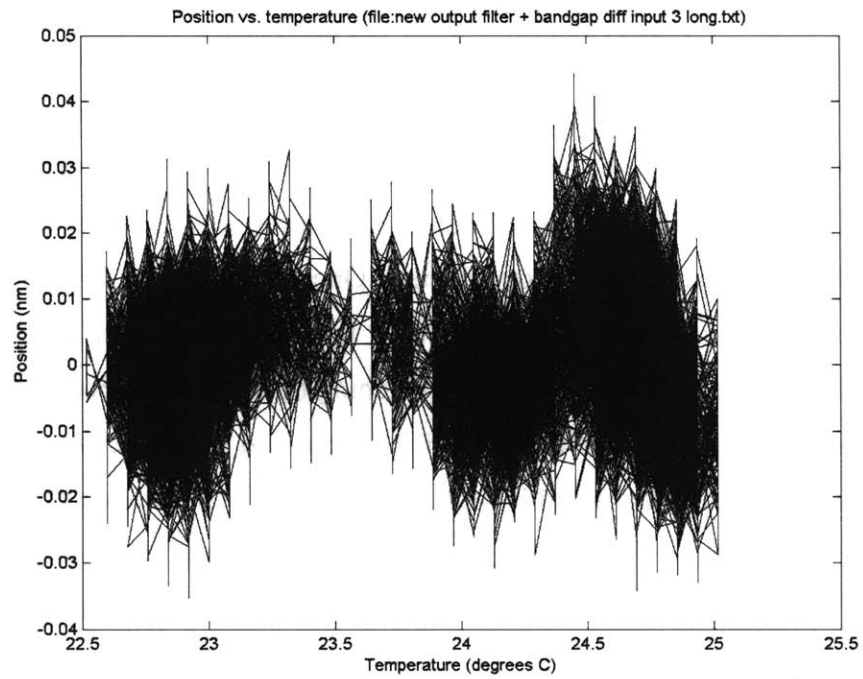
Figure 30: Temperature dependence of drift from bandgap reference and output filter
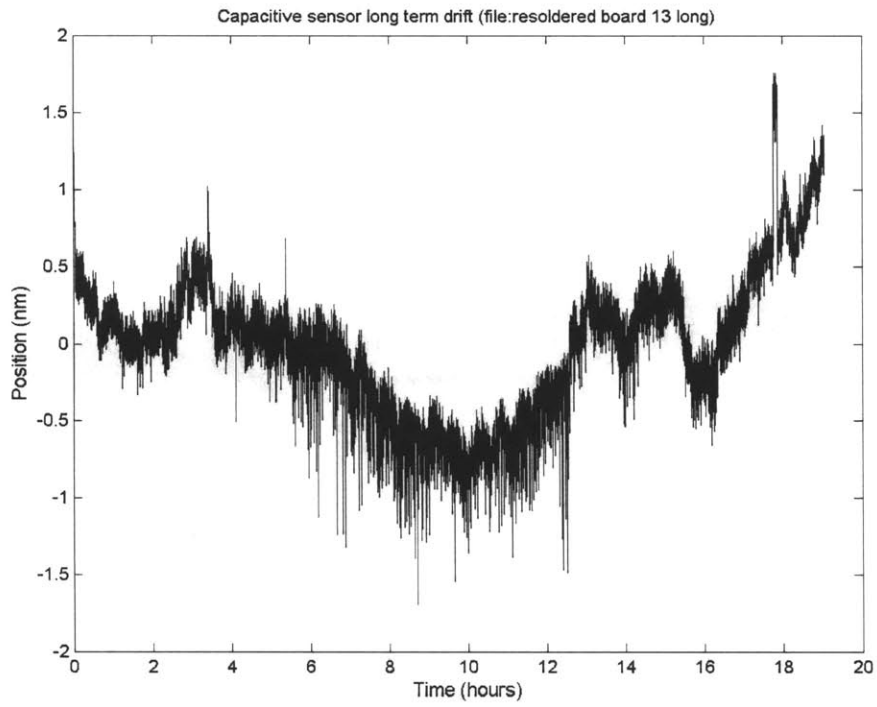
Figure 31: System output without calibration
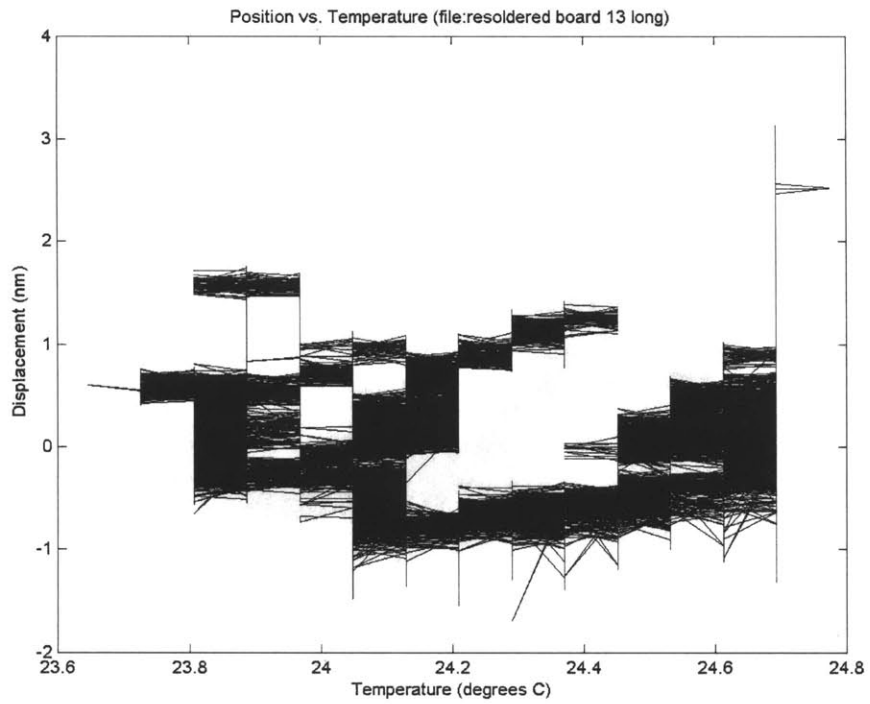
Figure 32: Temperature dependence of drift

57
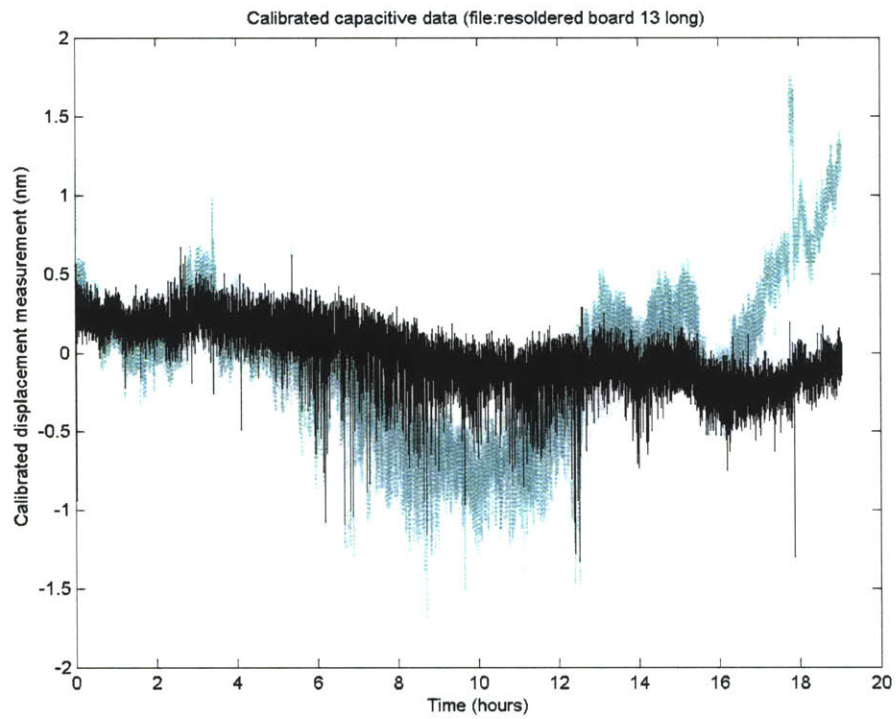
Figure 33: System output with calibration showing less than 1nm drift
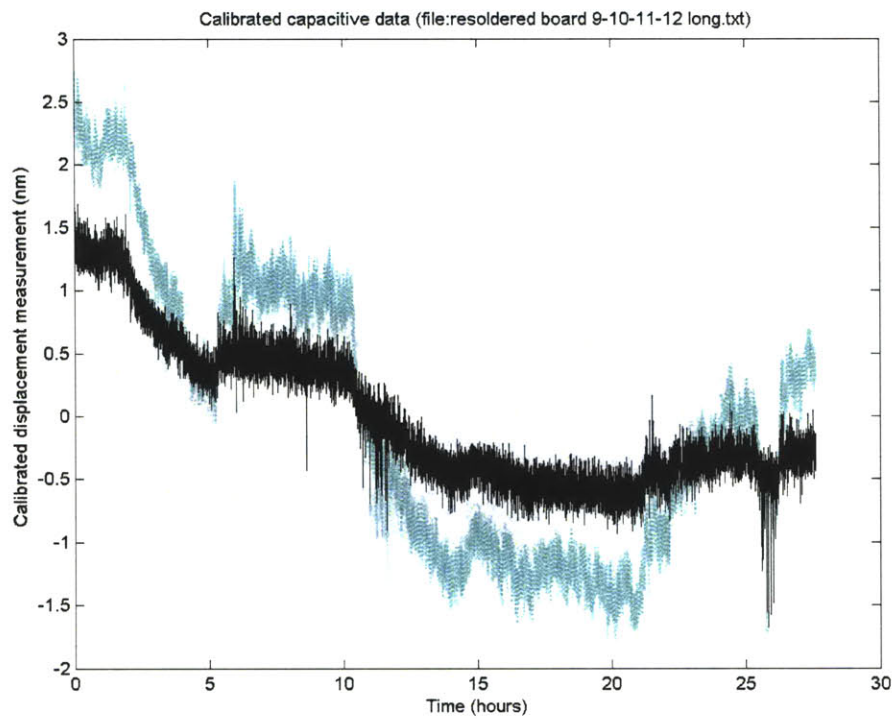
Figure 34: System output with calibration in the presence of external disturbances

5.4 Overall Error Budget

Table 2 shows the overall error budget of the system with an expected resolution of 0.2nm and long-term drift within 2nm.

Source	Measured noise RMS	Measured noise peak-to-peak	Expected resolution (RMS+PP)/2
Noise	0.056nm	0.3nm	0.2nm
Drift	1nm	1nm	1nm

Table 2: Overall error budget

6 Conclusion and Future Work

6.1 Conclusion

The objective of this work is to develop a displacement measurement system for the Nanogate with better than 1nm resolution and long-term stability with at least 100 Hz system bandwidth. The Nanogate is a circular cantilever structure that allows the precise control of the separation between ultra-flat silicon and Pyrex surfaces to form a tunable nanometer gap.

Several displacement sensing strategies are considered including techniques based on measuring optical intensity, optical phase, and capacitance. The capacitive technique is chosen for its ease of mechanical integration with the Nanogate and the capability to achieve high measurement resolution. To make the capacitive displacement sensing compatible with future fluid flow applications, the capacitive electrodes are placed at the outer edge of the circular silicon diaphragm and at the corresponding region on the Pyrex base. A Zygo interferometer displacement sensor can then be used to determine the mapping between capacitance and displacement of the gap.

A new version of the Nanogate is fabricated that incorporates the capacitive electrodes. The processing yield is increased by using silicon dioxide "hard" mask during DRIE and incorporating wafer level bonding into the fabrication process.

Electronics for capacitive sensing is developed to convert capacitance in the Nanogate to a voltage and then to a digital value. An analog front-end printed circuit board is designed and built that uses synchronous detection to produce a voltage output for the corresponding capacitance. A custom data acquisition system is developed to accurately digitize this voltage. The result is transmitted via serial line to a computer where the data is stored and graphed by a Visual Basic program. In order preserve the accuracy of the measurement, careful layout considerations are made in both circuit boards and a calibration scheme is introduced to reduce drift in the system.

In the final system, the Nanogate capacitance is found to vary linearly with displacement once the silicon and Pyrex surfaces are separated. The residue plot shows a

periodic fine structure on the order of 5nm, but more analysis is necessary to understand its physical origin.

The noise and drift of this measurement system has been optimized and tested. The expected resolution is 0.2nm with a system bandwidth of 160 Hz and an expected long-term drift of 1nm. The goals set out at the beginning of this thesis have been met, although careful consideration must be given to shielding and environmental control around the measurement system.

6.2 Future Work

In addition to adding an improving the calibration scheme discussed in the previous section, the next steps in obtaining true nanometer control of the gap separation is to develop a better actuator. Some of the basic requirements include better than nanometer open-loop resolution and the ability to apply a uniform force around the perimeter of the silicon diaphragm. An integrated actuator using piezoelectric material may have fewer packaging requirements and therefore be an attractive option. This work may be complemented by adding quadrant capacitive electrodes to measure uneven deflections on the silicon diaphragm.

The first application of the Nanogate will be for a portable gas transfer standard for the National Institute of Standards and Technology (NIST). This work will involve incorporating the improved sensor and actuator with gas tight fluid connections and calibrating the values of capacitance with a flow rate measured by a highly sensitive mass spectrometer.

One of the long-term goals of the Nanogate is the use the controllable nanometer gap as a tool for studying molecular behavior in highly confined spaces. This would require the nanometer gap to be filled with liquid, which means that the transfer function between capacitance at the outer edge and gap length will be dependent on the mechanical properties of the fluid in the gap. As result, this capacitive sensing geometry will probably not be feasible and a more direct sensing geometry is necessary. This could possibly involve mounting a capacitive electrode some distance away from the center of the silicon diaphragm.

Bibliography

1.	Chen, D.Y.C. and R.G. Horn, *The drainage of thin liquid films between solid surfaces.* J. Chem. Phys., 1985. **83**(10): p. 5311-5323.

2.	Demirel, A.L. and S. Granick, *Origins of solidification when a simple molecular fluid is confined between two plates.* J. Chem. Phys., 2001. **115**(3): p. 1498-1512.

3.	Zhu, Y. and S. Granick, *Rate dependent slip of Newtonian liquid at smooth surfaces.* Phys. Rev. Lett., 2001. **87**(9, 27).

4.	Zhu, Y. and S. Granick, *Limits of the hydrodynamic no-slip boundary condition.* Phys. Rev. Lett., 2002. **88**(10,11).

5.	Slocum, A.H., *Method of and apparatus for substance processing with small opening gates actuated and controlled by large displacement menbers having fine surface finishing.* 1999: US.

6.	White, J.R., et al., *An instrument to control parallel plate separation for nanoscale flow control.* Review of Scientific Instruments, 2003. **74**(11).

7.	White, J.R., *The Nanogate: Nanoscale Flow Control. Ph.D. Thesis,* in *Mechanical Engineering.* 2003, Massachusetts Institute of Technology.

8.	*Zygo ZMI-1000.*

9.	Ma, H. and J. White, *Packaging and Initial Characterization of the Nanogate.* 2001, Massachusetts Institute of Technology, MAS.962 final report: Cambridge.

10.	*APC International, www.americanpiezo.com.*

11.	Fraden, J., *Handbook of Modern Sensors: Physics, Designs, and Applications.* 2 ed. 1997: springer Verlag.

12.	*Keyence laser displacement sensor: http://www.keyence.com/products/measuring/lc/lc_spec.html.*

13.	*Zygo ZMI optical probe accessory manual, OMP-0238B.*

14.	Yaralioglu, G.G., et al., *Analysis and design of an interditial cantilever as a displacement sensor.* J. Appl. Phys., 1998. **12**(83): p. 7405-7415.

15.	Manalis, S.R., et al., *Interditial cantilevers for atomic force microscopy.* Appl. Phys. Lett., 1996. **69**(25): p. 3944-3946.

16. Puers, B., *Capacitive sensors: when and how to use them.* Sensors and Actuators, 1993. **A37-A38**: p. 93-105.

17. Jones, R.V. and J.C.S. Richards, *The design and some applications of sensitive capacitance micrometers.* Journal of Physics E: Scientific Instruments, 1973. **6**: p. 589-600.

18. Baxter, L., *Capacitive Sensors: Design and Applications.* IEEE Press Series on Electronics Technology. 1996: IEEE.

19. Paradiso, J.A., *New technologies for monitoring the precision alignment of large detector systems.* Nuclear Instruments and Methods in Physics Research A., 1997. **386**: p. 409-420.

20. *ADXL50 datasheet: http://www.analog.com/UploadedFiles/Obsolete_Data_Sheets/2044696ADXL50. pdf*, Analog Devices.

21. Khanna, R. 2003.

22. *Mark Optics.* www.markoptics.com

23. *OPA129 datasheet: http://www-s.ti.com/sc/ds/opa129.pdf*, Texas Instruments.

24. *AD630 datasheet: http://www.analog.com/UploadedFiles/Data_Sheets/129044951AD630_d.pdf*, Analog Devices.

25. *LT1007 Datasheet: http://www.linear.com/pdf/100737fb.pdf*, Linear Technology.

26. *LT1019 datasheet: http://www.linear.com/pdf/1019fcs.pdf*, Linear Technology.

27. Lancaster, D., *Active Filter Cookbook.* 2nd ed. 1995, Thatcher, AZ: Synergetics Press.

28. Horowitz, P. and W. Hill, *The Art of Electronics.* 2nd ed. 1989: Cambridge University Press.

29. *LTC2440 datasheet: http://www.linear.com/pdf/2440f.pdf*, Linear Technology.

30. *MPS430F149 datasheet: http://www-s.ti.com/sc/ds/msp430f149.pdf*, Texas Instruments.

31. *AD592 datasheet: http://www.analog.com/UploadedFiles/Data_Sheets/136700329AD592_a.pdf*, Analog Devices.

32. *Tra-Duct 2902 Silver Epoxy, www.tra-con.com/products/tpb.asp?product=2902, Tra-Con.*

Appendix A: Nanogate Masks
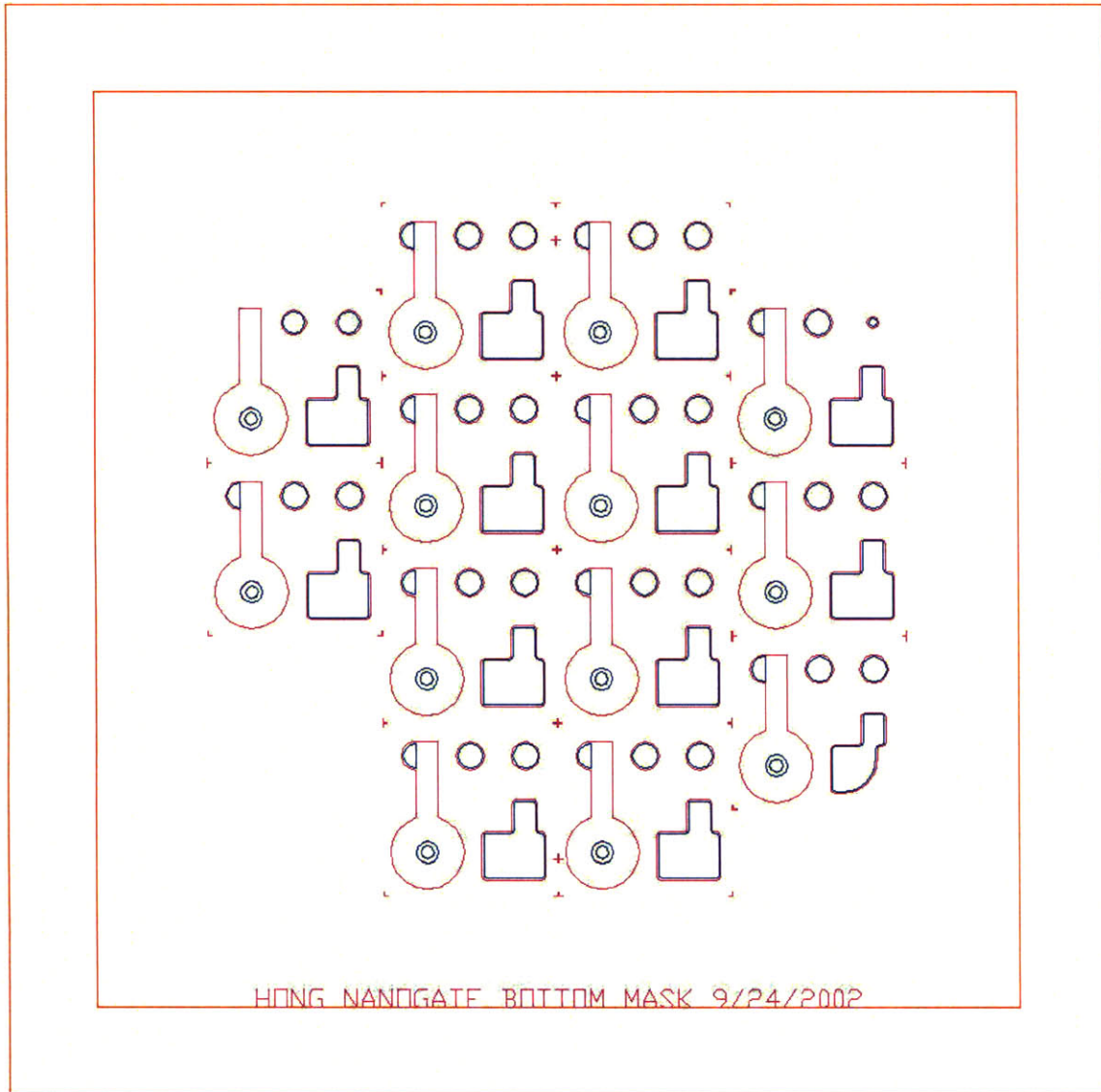
Figure 35: Mask for the Nanogate wafer bottom side (color inverted)
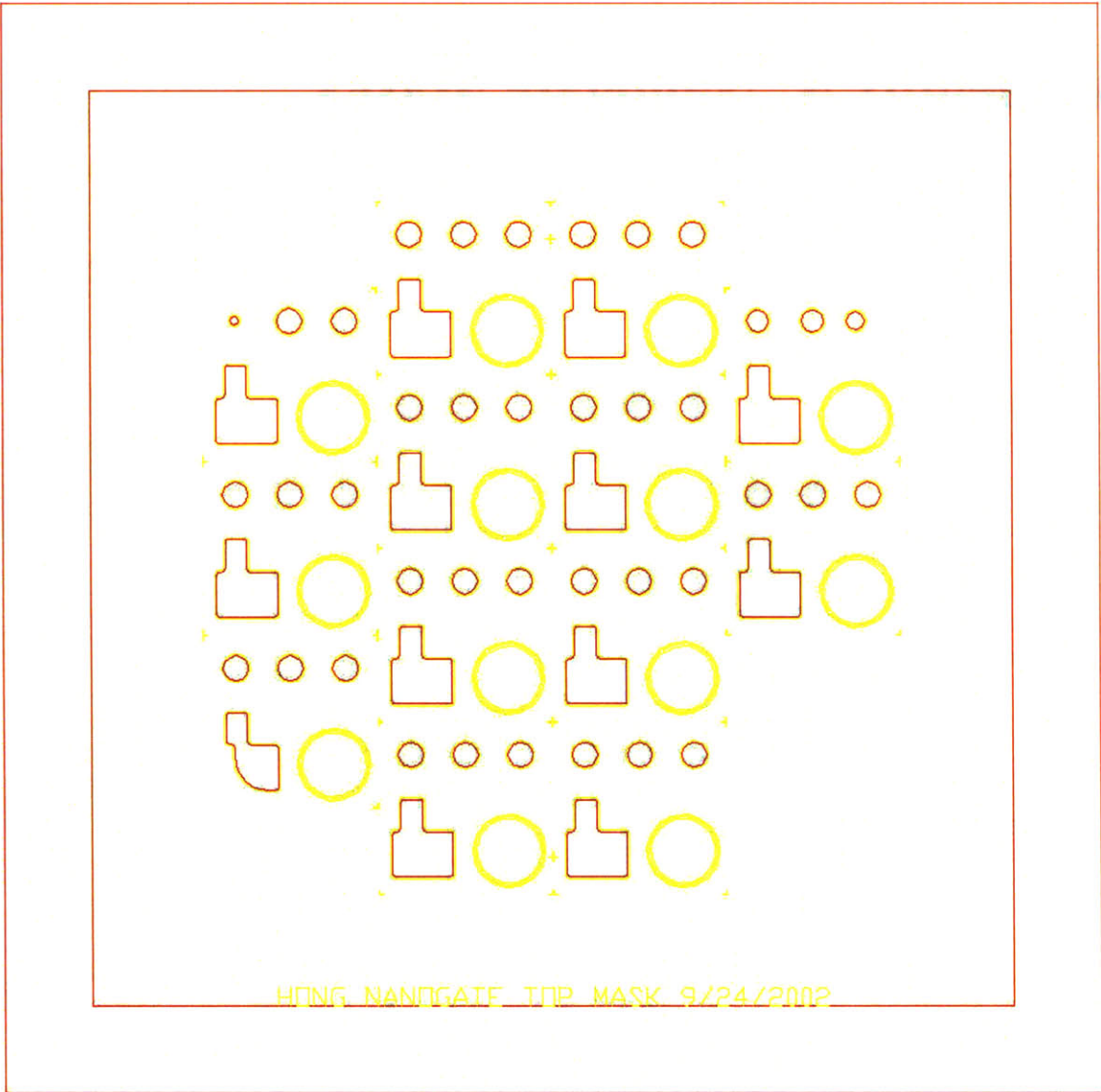
Figure 36: Mask for the Nanogate wafer top side (color inverted)

Figure 37: Mask for the Nanogate Pyrex base

Appendix B: Detailed Fabrication Process

Hongshen Ma
Created: December 29, 2002,
Updated: July 15, 2003
hongma@media.mit.edu

Meta Description	Description	Lab	Machine	Recipe	Diagram
Preparation and Oxidation	4", 500um heavily doped Si wafer. N-type, Sb doping, resistivity = 0.008 ohm-cm				Silicon Oxide Resist Gold Pyrex
	RCA	ICL	RcaTRL	SOP	
	Oxidation	ICL	Tube5D-fieldox	Grow 1um oxide, 1050 C, 200 min	
Top side pattern and etch	HMDS	TRL	HMDS	Recipe 3	
	Deposit thick resist	TRL	Coater	10um, AZ4620, 1500rpm	
	Prebake	TRL	Prebake	90°C, 60min	
	Expose	TRL	EV1	Expose 30s	
	Develop	TRL	Photo Wet	AZ440 2minutes per wafer	
	Rinse	TRL	Dump rinse	5min	
	Dry	TRL	SRD 4"		
	Coat backside	TRL	Coater	1um, OCG825, 3000rpm	
	Postbake	TRL	Postbake	90°C, 30min	
	Remove oxide	TRL	Acid-hood	BOE 16 minutes	
	Mount on 6" quartz carrier wafer	TRL	Coater	Target mount, AZ4620 1800 rpm	
	Alignment mark etch	TRL	STS-2	13s	

69

		Cover alignment mark	TRL	photoroom	Use AZ4620 and q-tip bake for 5min	
		DRIE	TRL	STS-2	Etch 170-190um, MIT37A 50 minutes	
		Remove Teflon	TRL	Asher	20+ minutes	
		Dismount	TRL	Acidhood2	Piranha X 2 (or more)	
	Bottom side pattern and etch	HMDS	TRL	HMDS	Recipe 3	
		Deposit thick resist	TRL	Coater	10um, AZ4620, 1500rpm	
		Prebake	TRL	Prebake	90°C, 60min	
		Expose	TRL	EV1	Expose 30s	
		Develop	TRL	Web bench	AZ440 2minutes per wafer	
		Rinse	TRL	Dump rinse		
		Dry	TRL	SRD 4"		
		Coat backside	TRL	Coater	1um, OCG825, 3000rpm	
		Postbake	TRL	Postbake	90°C, 60min	
		Remove oxide	TRL	Acidhood	BOE 16 minutes	
		Mount on 6" quartz carrier wafer	TRL	Coater	Target mount, AZ4620, 1800 rpm	
		Alignment mark etch	TRL	STS-2	13s	
		Cover alignment mark	TRL	photoroom	Use AZ4620 and q-tip bake for 5min	
		DRIE	TRL	STS-2	Etch 150um use MIT37A 50 minutes or until through	
		Remove Teflon	TRL	Asher	20+ minutes	
		Dismount	TRL	Acid-hood	Piranha X 2 (or more)	
	Add bond stop layer and metal	Deposit electrode	TRL	E-beam	20nm Ti, 100nm Au	
		Mount shadowmask	TRL	Photo room	***Use a small amount of AZ4620 resist	

contacts	Bake	TRL	Prebake	90°C, 10 minutes	
	Deposit metal	TRL	E-beam	20nm Ti, 100nm Pt, 20nm Ti, 100nm Au	
	Acetone dismount	TRL	Photowet	As long as needed	
	Solvent clean	TRL	Photowet	Methenol and Isopropanol	
	DI-water clean	TRL	Dump rinse		
	Dry	TRL	SRD 4"		
Process for electrical traces on Pyrex base. We use 500um Pyrex 7740 wafer	HMDS	TRL	HMDS		
	Deposit Photoresist	TRL	Coater	1um OCG825 resist	
	Prebake	TRL	Prebake	90°C, 30 minutes	
	Exposure	TRL	EV-1	2s	
	Develop	TRL	Photo wet	AZ440	
	Postbake	TRL	Postbake	120°C, 30 minutes	
	Remove residual resist	TRL	asher	2 min	
	Deposit metal	TRL	eBeamAu	20nm Ti, 80nm Al	
	Liftoff	TRL	Photo wet	Acetone overnight	
	Solvent clean	TRL	Photowet	Methenol and Isopropanol	
	DI-water clean	TRL	Dump rinse		
	Dry	TRL	SRD 4"		
Anodic bond	Anodic bond	TRL	EV501-620	325°C, 1000N, 600V–5min, 800V-30min	
Diesaw	Diesaw	ICL	diesaw		

Appendix C: Circuit Diagrams and PCB Layout
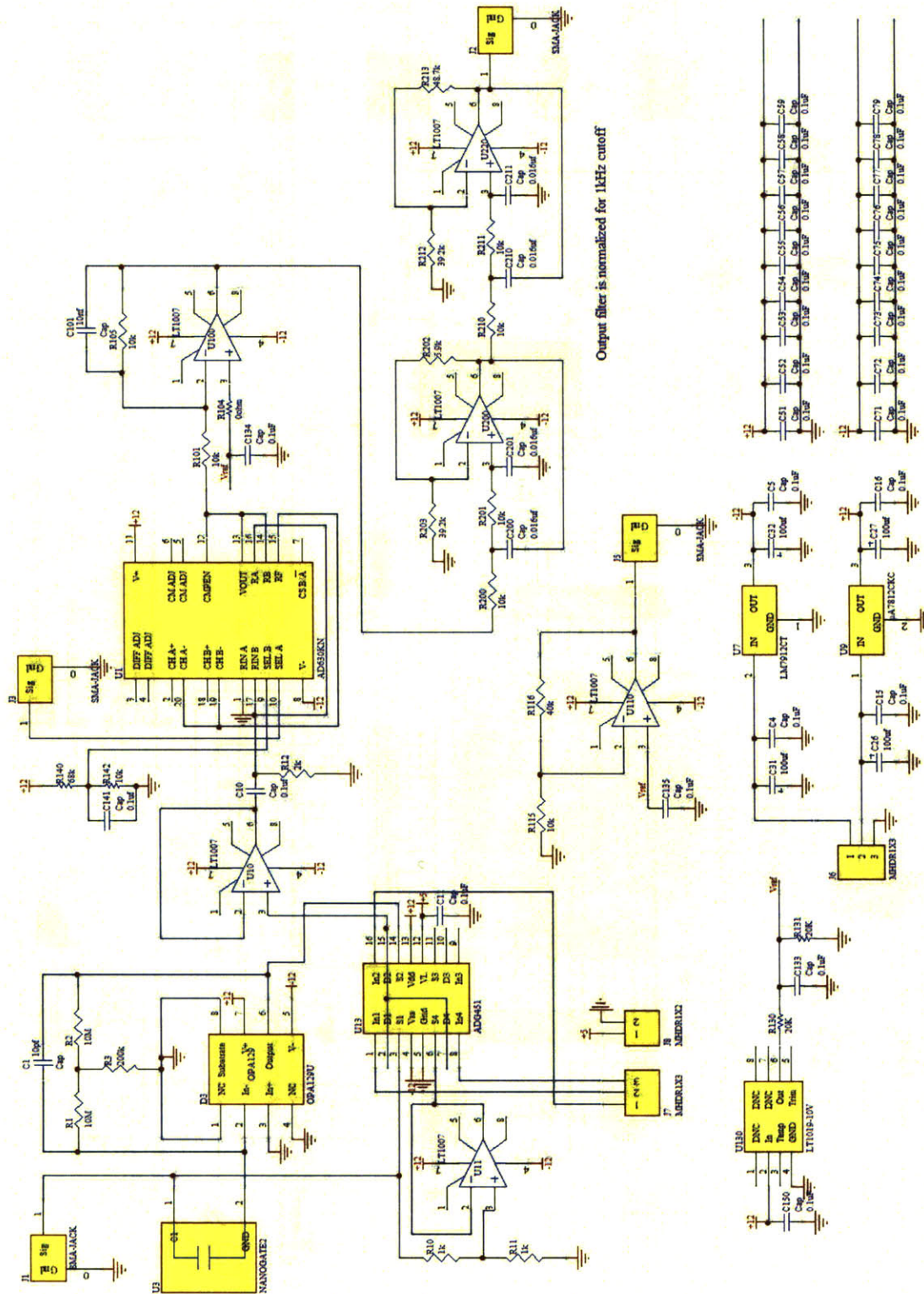
Figure 38: Analog front-end full schematic
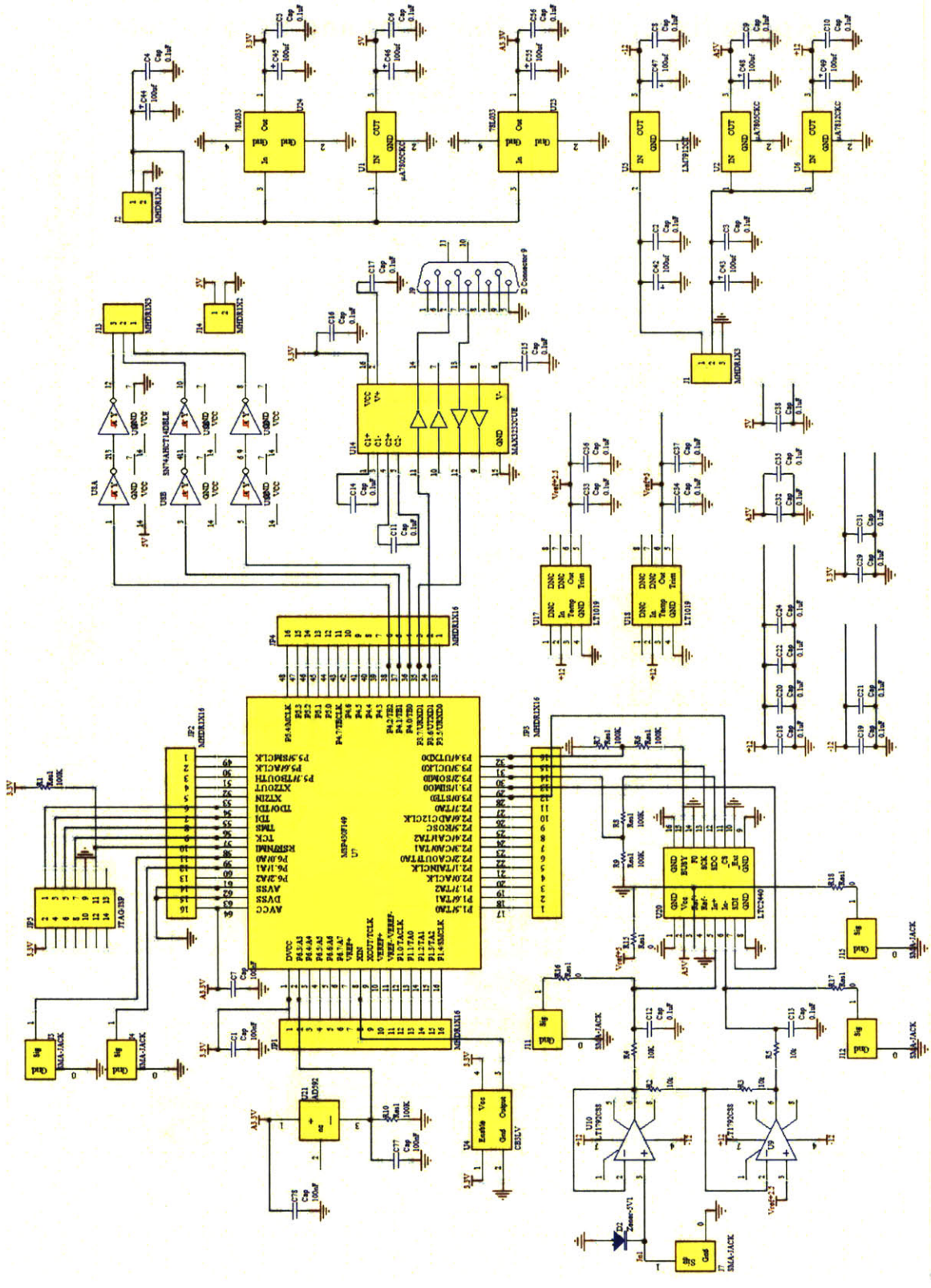
Figure 39: Data acquisition circuit full schematic
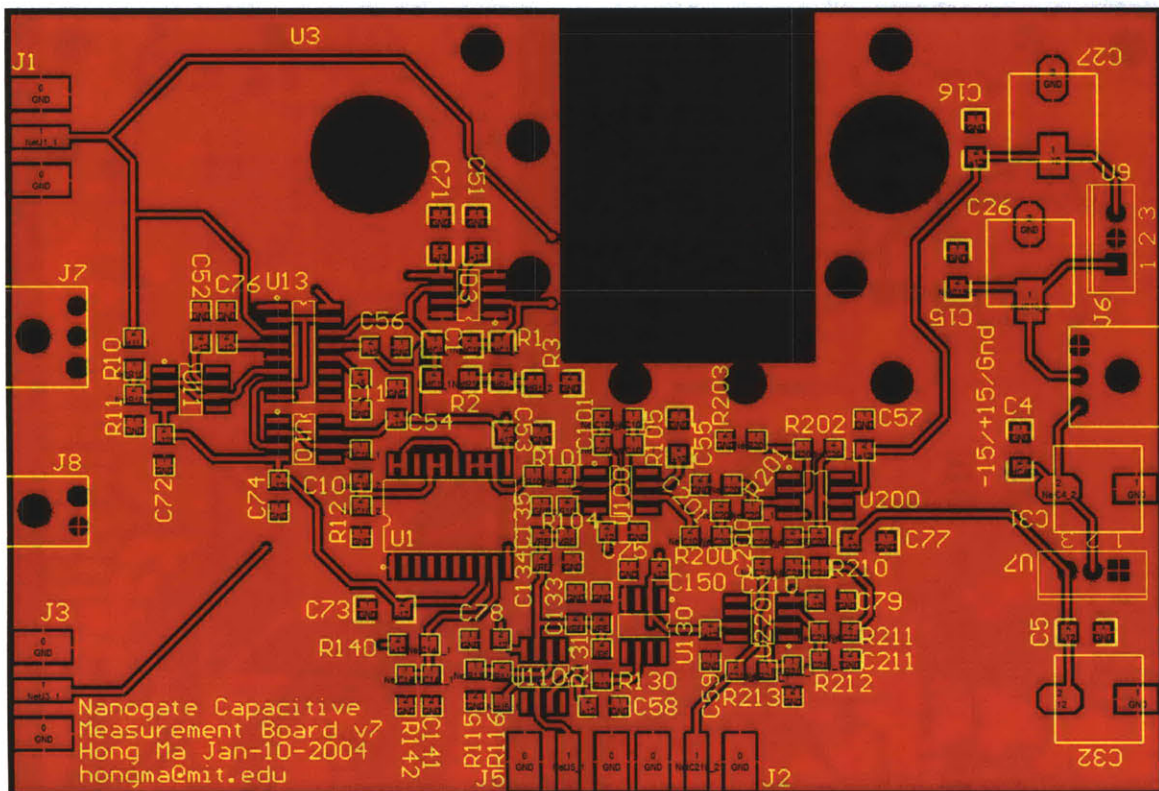
Figure 40: Analog front-end PCB layout, top layer
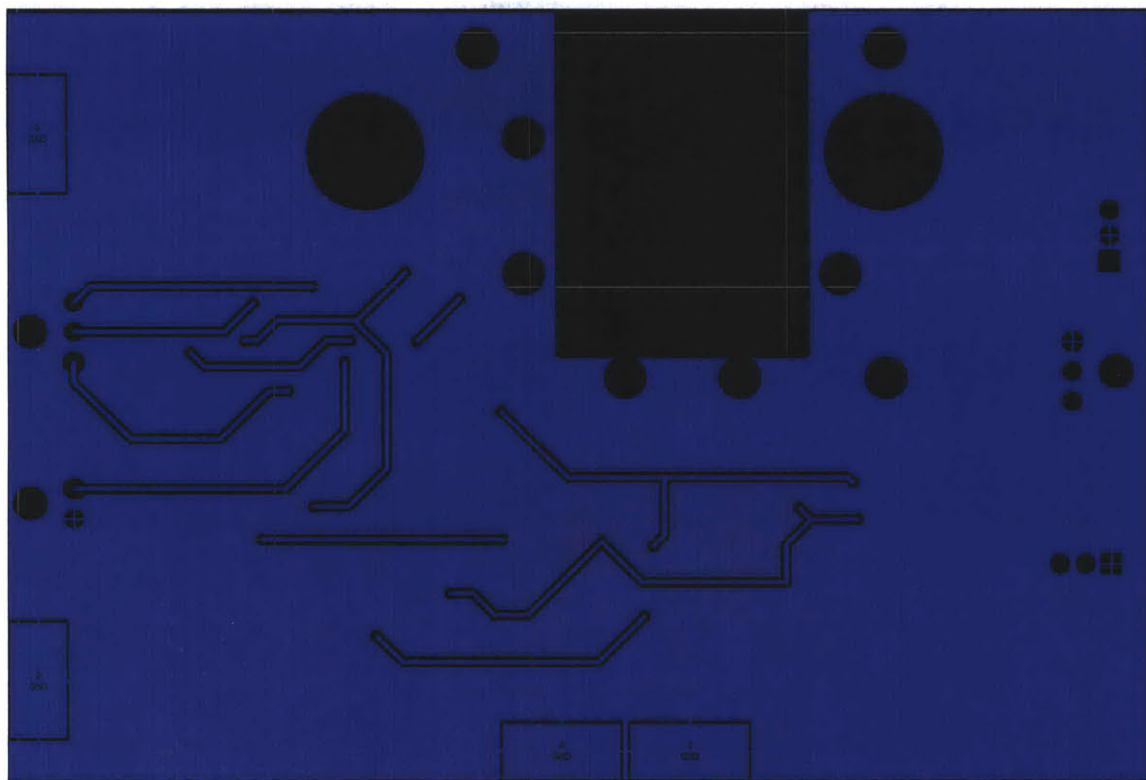
Figure 41: Analog front-end PCB layout, bottom layer
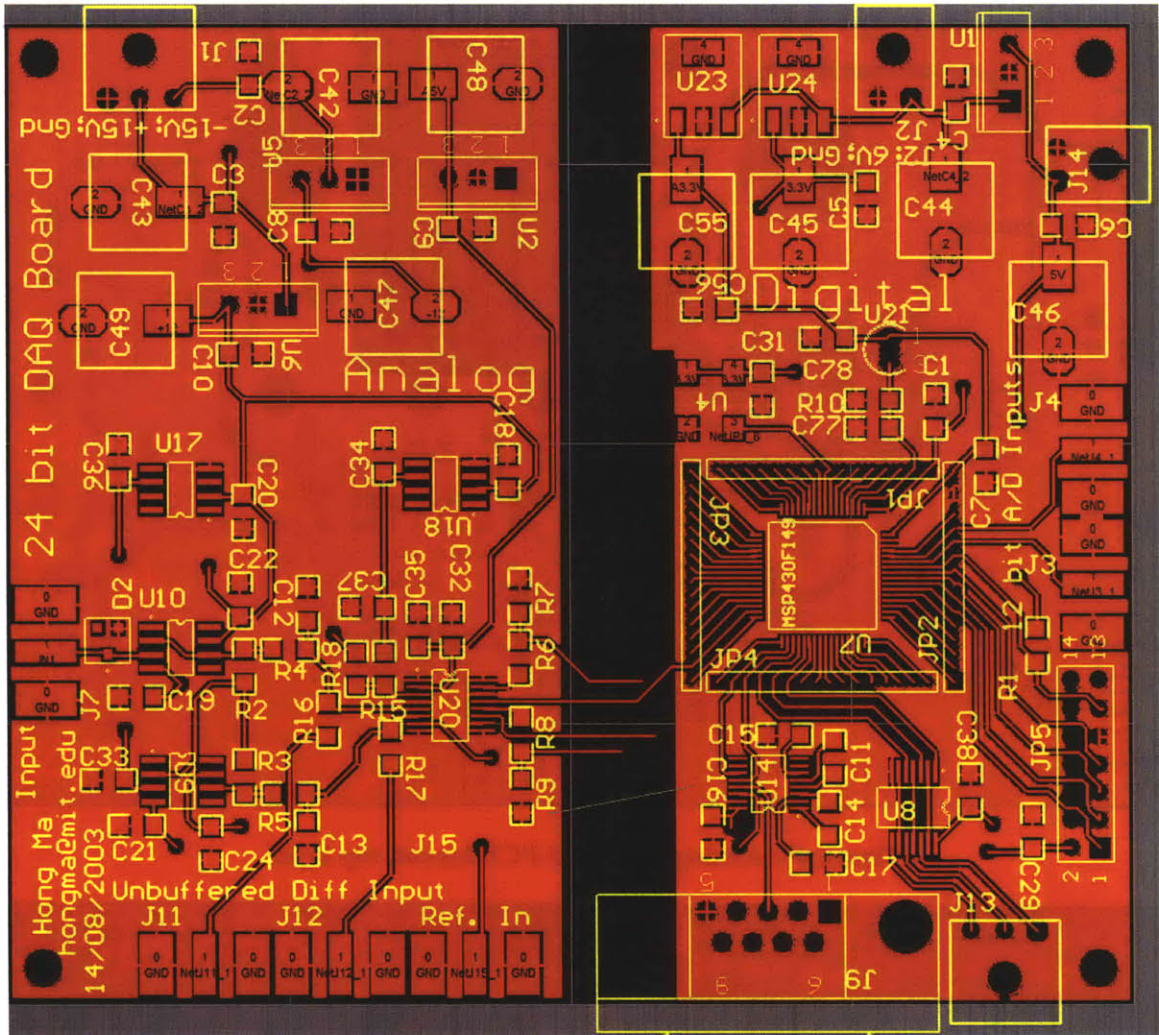
Figure 42: Data acquisition PCB layout, top layer
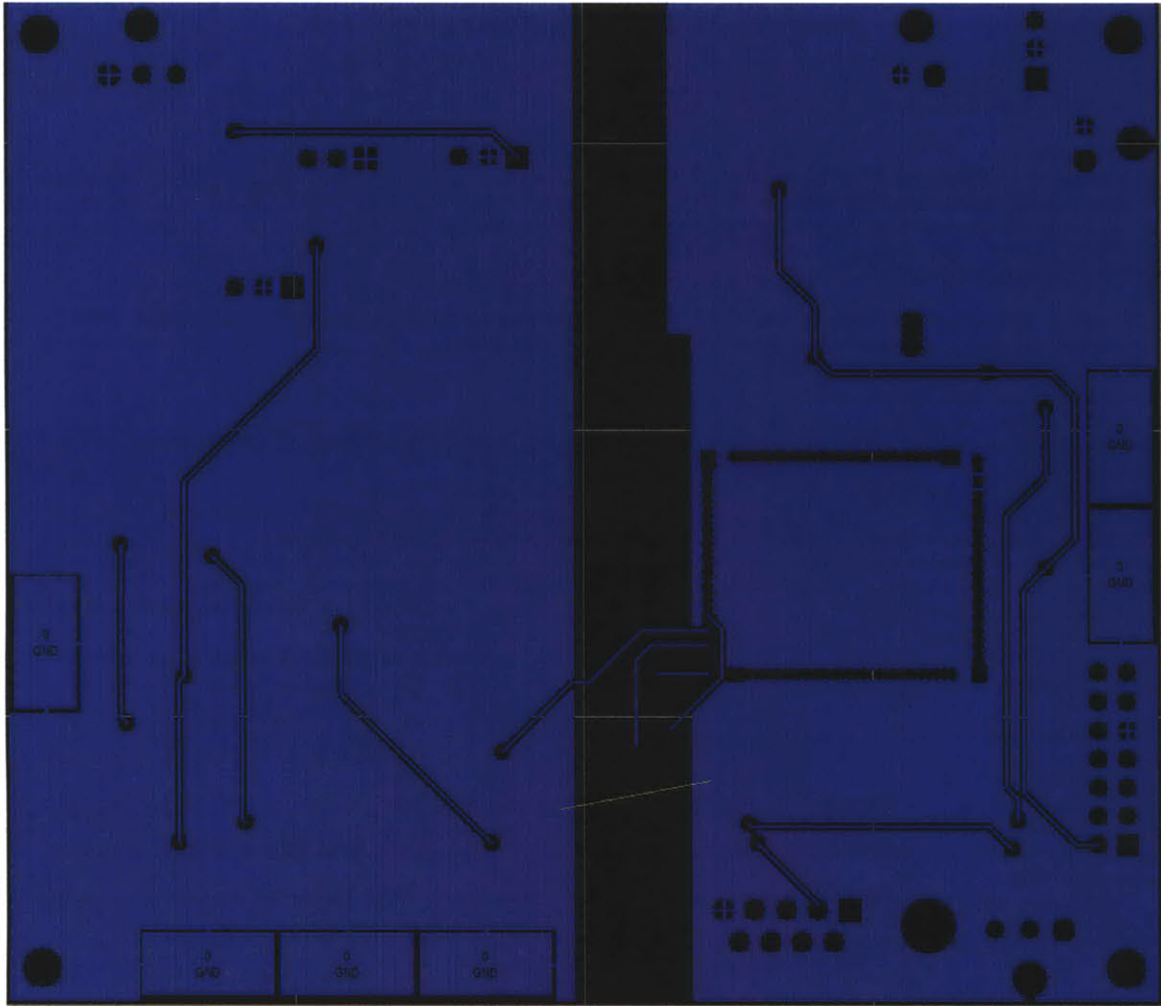
Figure 43: Data acquisition PCB layout, bottom layer

Appendix D: MSP430 Microprocessor Code

```
//*****************************************************************
// MSP430F149 interface for LTC2440 ADC
//
// Hongshen Ma
// Created: August 28, 2003
// Last modified: Jan. 20, 2004
//*****************************************************************

#include <msp430x14x.h>

//#define OSR (0x30000000)              // OSR value determines ADC conversion rate
//unsigned long int OSRbuf = OSR; // OSR shift register
unsigned long int capdata = 0;
unsigned long int buf32 = 0;
unsigned char buf8=0;
unsigned int picostate=0;           // 0 waiting for instruction, 1 processing
instruction, 2 turning picomotor
unsigned int picosteps;             // number of steps
char picostat='A';                  // A no step; B CW step; C CCW step
unsigned int picotime=0;             // keeps track of timer cycles
signed char stepsdone=0;
unsigned int tempsense;             // 12bit temperature value in Kelvins
unsigned int calmode=0;              // calibration mode indicator: 0=normal
operation, 1=baseline calibration, 2=scalefactor calibration
unsigned int calcount=3;          //calibration counter, we plan to make a calibration
once a minute = every 1200 counts

void main(void)
{
  unsigned int i;
  WDTCTL = WDTPW + WDTHOLD;          // Stop WDT: required
//clock settings
  BCSCTL1 = XTS + XT2OFF + RSEL0 + RSEL1 + RSEL2;   // Enable XT1, disable XT2, highest
possible DCO
  BCSCTL2 = SELM1 + SELM0;        // MCLK = XT1, SMCLK=DCO, DCO internal resistors, SMCLK
divide by 1
  do
  {
  IFG1 &= ~OFIFG;                   // Clear OSCFault flag
  for (i = 0xFF; i > 0; i--);       // Time for flag to set
  }
  while ((IFG1 & OFIFG) != 0);       // OSCFault flag still set?

//serial communication settings 57600 baud on USART1
//UART1 -> PC
  U1CTL = CHAR;                      // 8-bit character
  UTCTL1 = SSEL0;                    // UCLK = ACLK
  U1BR0 = 0x8B;                      // Set PC UART Baud rate
  U1BR1 = 0x00;                      // at 57.6k baud
  UMCTL1 = 0x00;                     // no modulation
  ME2 |= UTXE1 + URXE1;             // Enable USART0 TXD/RXD
  IE2 |= URXIE1;                    // Enable USART0 RX interrupt
  P3SEL |= BIT6 + BIT7;             // P3.4,5 = USART0 TXD/RXD
  P3DIR |= BIT6;                    // P3.4 output direction

//internal ADC settings
  ADC12CTL0 = ADC12ON;            // Turn on ADC12, use int. 1.5V reference
  ADC12CTL1 = ADC12SSEL_2;             // Use MCLK for ADCCLK
  ADC12MCTL0 = INCH_3;           // Select input and reference channels
  P6SEL |= BIT3;                     // Enable A6

//Port settings for Picomotor driver
  P4DIR |= BIT0 + BIT1 + BIT2;         // BIT0=CLK, BIT1=DIR, BIT2=STEP
//Pin settings for LTC2440 ADC
//P3.0=_CS; P3.1=SDI; P3.2=SDO; P3.3=SCK; P3.4=BUSY
  P3DIR |= BIT0 + BIT1 + BIT3;
  P3OUT = BIT0;
  P5DIR |= BIT0 + BIT1 + BIT3;
```

```c
  P5OUT = BIT0 + BIT1 + BIT2;

//TimerA and TimerB settings
  TACTL = TASSEL0 + TACLR + MC0;          // Timer A clocking on ACLK, up count mode, clear
interrupt
  TACTL &= ~TAIFG;

  TBCTL = TBSSEL0 + TBCLR + MC0 + ID_3;       // Timer B use ACLK, clear TAR, upcount mode
  TBCCTL0 = CCIE;                         // CCR0 interrupt enabled
  TBCCR0 = 50000;                         // Run Timer B at 20Hz

  _EINT();                                // Enable interrupts

  for (;;)
    {
    _NOP();                               // Required only for C-spy
    }
}

interrupt[TIMERB0_VECTOR] void Timer_B (void)
{
  unsigned int i;

if (picotime == 1)
{
  while (P3IN & BIT4);
  P3OUT &= ~BIT0;
  _NOP();
  _NOP();
  while (P3IN & BIT2);
//  OSRbuf = OSR;

//if we are ready for a calibration we switch over to the calibration input
  if ((calcount % 150)==0)     // First calibration mode
    {
    P5OUT = BIT0 + BIT1 + BIT2;
    for (i=1;i<=10;i++);
    calcount=0;
    calmode=0;                       // Here calmode is actually 0 since this result will be
ADC'ed in the next round.
    P5OUT = BIT0 + BIT2;
    for (i=1;i<=1000;i++);
    }
  else if (((calcount % 150)>=1) && ((calcount % 150)<=22))
    {
    calmode=1;
    }
  else if ((calcount % 150)==23)
    {
    P5OUT = BIT0 + BIT1 + BIT2;
    for (i=1;i<=10;i++);
    calmode=1;
    P5OUT = BIT1 + BIT2;
    }
  else if ((calcount % 150)==24)
    {
    calmode=1;                       // We can only report the calibration later because of the
1 data point buffer in the ADC
    }
  else
    {
    calmode=0;
    }
  calcount++;

//now we get data from the A/D converter
  for (i=1;i<=32;i++)
    {
      P3OUT |= BIT3;
      _NOP();
      //read in data
```

```
        capdata=capdata << 1;
        buf32 = P3IN & BIT2;
        capdata |= buf32 >> 2;
        P3OUT &= ~BIT3;
        _NOP();
        //set speed
//        P3OUT |= (OSRbuf & 0x80000000) >> 30;
//        OSRbuf = OSRbuf << 1;
    }
   P3OUT |= BIT0;                    // Start next conversion

// read from temp sensor
   ADC12CTL0 |= ADC12SC + ENC;        // Sampling open
   ADC12CTL0 &= ~ADC12SC;             // Sampling closed, start conversion
   while ((ADC12CTL1 & ADC12BUSY) == 1);   // ADC12BUSY?
   tempsense = ADC12MEM0;             // get conversion results

// finished now transmit data over UART
   capdata = capdata << 3;
   buf8 = (capdata & 0xFF000000) >> 24;
   while ((IFG2 & UTXIFG1) == 0);         // USART0 TX buffer ready?
   TXBUF1 = buf8;
   buf8 = (capdata & 0x00FF0000) >> 16;
   while ((IFG2 & UTXIFG1) == 0);         // USART0 TX buffer ready?
   TXBUF1 = buf8;
   buf8 = (capdata & 0x0000FF00) >> 8;
   while ((IFG2 & UTXIFG1) == 0);         // USART0 TX buffer ready?
   TXBUF1 = buf8;
   while ((IFG2 & UTXIFG1) == 0);         // USART0 TX buffer ready?
//We use to use this bit to indicate steps done by the pico motor
   TXBUF1 = stepsdone + '0';
   stepsdone=0;
//temperature data
   buf8 = (tempsense & 0x0F00) >> 8;
   while ((IFG2 & UTXIFG1) == 0);         // USART0 TX buffer ready?
   TXBUF1 = buf8;
   buf8 = tempsense & 0x00FF;
   while ((IFG2 & UTXIFG1) == 0);         // USART0 TX buffer ready?
   TXBUF1 = buf8;
//previousely we transmitted the 'K' character but now...
//We use this bit to indicate the state of the calibration
//'0' indicate normal operation, '1' indicate baseline calibration, '2' indicate scale
factor calibration
   while ((IFG2 & UTXIFG1) == 0);         // USART0 TX buffer ready?
   TXBUF1 = '0' + calmode;
}

// Picomotor driver
   P4OUT ^= BIT0;                        // 500 Hz clock for picomotor
   if (picostate==4)
     {
     P4OUT ^= BIT2;
     if ((P4OUT & BIT2)==0)
       {
       picosteps--;
       if (P4OUT & BIT1)
         {
           stepsdone++;
         }
       else
         {
           stepsdone--;
         }
       }
     if (picosteps<=0)
       {
       picostate=0;
       }
     }
picotime++;
picotime = picotime % 8;
```

```
}

interrupt[UART1RX_VECTOR] void usart1_rx (void)
{
  char temp;
  temp = RXBUF1;
  if ((picostate==0) && (temp=='C'))
    {
    P4OUT |= BIT1;
    picostate=1;
    }
  else if ((picostate==0) && (temp=='D'))          //CCW
    {
    P4OUT &= ~BIT1;
    picostate=1;
    }
  else if (picostate==1)
    {
    picosteps=temp*256;
    picostate=2;
    }
  else if (picostate==2)
    {
    picosteps=picosteps + temp;
    picostate=3;
    if (picosteps > 2000)
      {
      picosteps = 2000;
      }
    }
  else if (picostate==3)
    {
    if (temp=='X')
      picostate=4;
    }
  else if ((temp=='*') && (picostate==0))          //restart condition
    { CCR0 = 65000;                                // After synchronization signal wait
15*clk for MSB
      TACTL |= TACLR;                              // Timer operation
      TACTL &= ~TAIFG;                             //
      while (!(TACTL & TAIFG));
    }
  else
    {
    picostate=0;
    }
}
```

Appendix E: Visual Basic Data Acquisition Program

```
Option Explicit
Dim holdover As String
Dim holdzygo As String
Dim recordflag As Boolean
Dim numerror As Long
Dim capdata As Double
Dim tempdata As Double
Dim zygodata As Double
Dim picodata As Long
Dim caldata As String
Dim scriptflag1 As Boolean
Dim scriptbuf As String
Dim command As String
Dim cycles As Integer
Dim delimiter As Integer
Dim savefilename As String


Private Sub crc_Click()
Dim i As Integer
Dim j As Integer
Dim crcData As String
crcData = "hon"
Dim crcReg As Byte
Dim databyte As Byte
crcReg = 255
Dim CRC8_poly As Byte
CRC8_poly = 24
Dim temp As Byte


For j = 1 To Len(crcData)
    databyte = Asc(Mid(crcData, j, 1)) 'or something
    For i = 1 To 8
        If ((crcReg And 128) Xor (databyte And 128)) <> 0 Then
            temp = crcReg And 128
            crcReg = ((crcReg * 2) Mod 256) Xor CRC8_poly
        Else
            crcReg = ((crcReg * 2) Mod 256)
        End If
        databyte = (databyte * 2) Mod 256
    Next
Next
crcData = crcData + Chr$(crcReg)
crcReg = 255
For j = 1 To Len(crcData)
    databyte = Asc(Mid(crcData, j, 1)) 'or something
    For i = 1 To 8
        If ((crcReg And 128) Xor (databyte And 128)) <> 0 Then
            crcReg = ((crcReg * 2) Mod 256) Xor CRC8_poly
        Else
            crcReg = (crcReg * 2) Mod 256
        End If
        databyte = (databyte * 2) Mod 256
    Next
Next

End Sub

Private Sub continuous_Click()
continuous.Value = True
programmed.Value = False
Frame1.Enabled = False
Record1.Enabled = True
picoframe.Enabled = True
End Sub

Private Sub Form_Load()
```

```
Dim temp As String
holdover = ""
MSComm1.CommPort = 2
MSComm1.Settings = "57600,n,8,1"
MSComm1.PortOpen = True
MSComm2.CommPort = 1
MSComm2.Settings = "19200,n,8,1"
MSComm2.PortOpen = True
Timer1.Interval = 50
Record1.Enabled = True
recordflag = False
Frame1.Enabled = False
programmed.Value = False
continuous.Value = True
numerror = 0
picodata = 0
CW.Value = True
CCW.Value = False
scriptflag1 = False
cycles = 0
delimiter = 0
command = ""
scriptbuf = ""

scriptexample.Caption = "Enter up, down, or wait" + Chr$(13) _
    + "plus number of cycles" + Chr$(13) + "each cycle equals 4ms" _
    + Chr$(13) + Chr$(13) + "For example:" + Chr$(13) + Chr$(13) _
    + "wait 100" + Chr$(13) + "down 50" + Chr$(13) + "wait 100" _
    + Chr$(13) + "up 20" + Chr$(13) + "wait 100"
logfilelabel.Caption = "Enter path and file name" + Chr$(13) _
    + "e.g. c:\data\log1" + Chr$(13) + "3 digit extension added automatically"
Call logfilename_Change

currentdata.Text = "hello!"
Strip1.MaxBufferSize = 1000
Strip1.VariableLastX = 1
Strip1.VariableDeltaX = 1
Strip1.XSpan = 1000
Strip1.ClearAll
Strip2.MaxBufferSize = 1000
Strip2.VariableLastX = 1
Strip2.VariableDeltaX = 1
Strip2.XSpan = 1000
Strip1.ClearAll
'MSComm1.Output = "*"            'reset TI microprocessor
MSComm1.InputLen = 0
temp = MSComm1.Input
MSComm2.InputLen = 0
temp = MSComm2.Input
End Sub
Private Sub Form_Unload(Cancel As Integer)
Dim temp As String

    MSComm1.InputLen = 0
    temp = MSComm1.Input
    MSComm2.InputLen = 0
    temp = MSComm2.Input
    If recordflag Then
        Print #3, "/* Halted at " + Str$(Now) + "*/"
        Close #3
    End If
    MSComm1.PortOpen = False
    MSComm2.PortOpen = False

End Sub

Private Sub logfilename_Change()
Dim filenumber As Integer
Dim ext As String
filenumber = 1
ext = "001"
```

```
Do Until Dir$(logfilename.Text + "." + ext) = ""
    filenumber = filenumber + 1
    ext = Format$(filenumber, "#")
    If Len(ext) = 1 Then
        ext = "00" + ext
    ElseIf Len(ext) = 2 Then
        ext = "0" + ext
    End If
Loop
logfileext.Text = ext
savefilename = logfilename.Text + "." + ext
End Sub

Private Sub MSComm1_OnComm()
    Dim buf As String
    Dim i As Integer
    Dim j As Integer
    Dim crcReg As Byte
    Dim databyte As Byte
    crcReg = 255
    Dim CRC8_poly As Byte
    CRC8_poly = 24

    'RECEIVE COMPLETE PACKET
        Dim Bits As String
        Dim holdCh As String
        Dim foostr As String
        Dim tmpState As Integer
        Dim DataFound As Boolean
        Dim holdInt As Integer
        Dim holdByte As Byte
        DataFound = False

    Select Case MSComm1.CommEvent
    ' Handle each event or error by placing
    ' code below each case statement

    ' Errors
        Case comEventBreak    ' A Break was received.
        Case comEventFrame    ' Framing Error
        Case comEventOverrun   ' Data Lost.
        Case comEventRxOver   ' Receive buffer overflow.
        Case comEventRxParity   ' Parity Error.
        Case comEventTxFull    ' Transmit buffer full.
        Case comEventDCB    ' Unexpected error retrieving DCB]

    ' Events
        Case comEvCD    ' Change in the CD line.
        Case comEvCTS    ' Change in the CTS line.
        Case comEvDSR    ' Change in the DSR line.
        Case comEvRing    ' Change in the Ring Indicator.
        Case comEvReceive    ' Received RThreshold # of
                            ' chars.
                MSComm1.InputLen = 1
                buf = MSComm1.Input
                holdover = holdover + buf
                If Len(holdover) = 7 Then
                    Call decodepacket
                    holdover = ""
                End If
        Case comEvSend    ' There are SThreshold number of
                        ' characters in the transmit
                        ' buffer.
        Case comEvEOF    ' An EOF charater was found in
                        ' the input stream
    End Select
End Sub
Private Sub MSComm2_OnComm()
    Dim buf As String
```

84

```
'RECEIVE COMPLETE PACKET
    Dim Bits As String
    Dim holdCh As String
    Dim foostr As String
    Dim tmpState As Integer
    Dim DataFound As Boolean
    Dim holdInt As Integer
    Dim holdByte As Byte
    DataFound = False

Select Case MSComm2.CommEvent
' Handle each event or error by placing
' code below each case statement

' Errors
    Case comEventBreak    ' A Break was received.
    Case comEventFrame    ' Framing Error
    Case comEventOverrun   ' Data Lost.
    Case comEventRxOver    ' Receive buffer overflow.
    Case comEventRxParity   ' Parity Error.
    Case comEventTxFull    ' Transmit buffer full.
    Case comEventDCB    ' Unexpected error retrieving DCB]

' Events
    Case comEvCD    ' Change in the CD line.
    Case comEvCTS    ' Change in the CTS line.
    Case comEvDSR    ' Change in the DSR line.
    Case comEvRing    ' Change in the Ring Indicator.
    Case comEvReceive    ' Received RThreshold # of
                        ' chars.
            MSComm2.InputLen = 1
            buf = MSComm2.Input
            If buf = Chr$(10) Then
                Call decodezygo
                holdzygo = ""
            Else
                holdzygo = holdzygo + buf
            End If
    Case comEvSend    ' There are SThreshold number of
                     ' characters in the transmit
                     ' buffer.
    Case comEvEOF    ' An EOF charater was found in
                     ' the input stream
    End Select
End Sub
Private Sub decodepacket()
Dim startpos As Integer
Dim i As Integer
Dim j As Integer

'CRC checker
'Dim crcReg As Byte
'Dim databyte As Byte
'Dim CRC8_poly As Byte
'crcReg = 255
'CRC8_poly = 24
'For j = 1 To Len(holdover)
'    databyte = Asc(Mid(holdover, j, 1))
'    For i = 1 To 8
'        If ((crcReg And 128) Xor (databyte And 128)) <> 0 Then
'            crcReg = ((crcReg * 2) Mod 256) Xor CRC8_poly
'        Else
'            crcReg = ((crcReg * 2) Mod 256)
'        End If
'        databyte = (databyte * 2) Mod 256
'    Next
'Next
'If crcReg <> 0 Then
'    numerror = numerror + 1
'    errormsg.Text = "CRC fail! " + Str$(numerror) + " errors"
'End If
```

```
'end of CRC checker

capdata = CLng(256 ^ 2) * CLng(Asc(Mid(holdover, 1, 1))) + CLng(256) *
CLng(Asc(Mid(holdover, 2, 1))) + Asc(Mid(holdover, 3, 1))
    If capdata >= 2 ^ 23 Then
        capdata = capdata - 2 ^ 24  'convert from 24bit signed to 32bit signed long
    End If
'     tempdata = CLng(256) * CLng(Asc(Mid(holdover, startpos + 4, 1))) + Asc(Mid(holdover,
startpos + 5, 1))

'     capdata = Val("&H" + holdover)
'     If Mid(holdover, 4, 1) = "+" Then
'         picodata = picodata - 1           '"+" is CW which means we are pushing down
'     ElseIf Mid(holdover, 4, 1) = "-" Then
'         picodata = picodata + 1           '"-" is CCW, we are going up
'     End If

picodata = picodata + Asc(Mid(holdover, 4, 1)) - Asc("0")
If picodata > 2000000 Then
    picodata = 2000000
ElseIf picodata < -2000000 Then
    picodata = -2000000
End If

tempdata = (CLng(Asc(Mid(holdover, 5, 1))) * CLng(256) + CLng(Asc(Mid(holdover, 6, 1))))
* (330 / 4096) - 273

caldata = Mid(holdover, 7, 1)

Strip1.Y = capdata
currentdata.Text = Str$(capdata)
'StdDev.Text = Strip1.VariableVisibleStdDev(0)

Strip2.Y = zygodata
currentdata2.Text = Str$(Format(zygodata, "0.000"))

numout.Text = holdover
tempdisp.Text = Str$(tempdata)

    If scriptflag1 Then
        If cycles <= 0 Then  'parse more of the script
            If Len(scriptbuf) <= 2 Then
                scriptflag1 = False
                Frame1.Enabled = True
                picoframe.Enabled = True
                startdaq.Caption = "Start Data Aquisition"
                Print #3, "/* Halted at " + Str$(Now) + "*/"
                Close #3
                recordflag = False
                startdaq.Enabled = True
                Call logfilename_Change
            Else
                delimiter = InStr(scriptbuf, " ")
                command = Mid$(scriptbuf, 1, delimiter - 1)
                scriptbuf = Mid$(scriptbuf, delimiter + 1, Len(scriptbuf))
                delimiter = InStr(scriptbuf, Chr$(13))
                cycles = Val(Mid$(scriptbuf, 1, delimiter - 1))
                scriptbuf = Mid$(scriptbuf, delimiter + 2, Len(scriptbuf))
                Select Case command
                    Case Is = "up"
                        Call runpico(cycles, False)
                    Case Is = "down"
                        Call runpico(cycles, True)
                    Case Is = "temp"
                        MSComm1.Output = "T"
                        cycles = 0
                Case Else
                End Select
                Print #3, "/* " + command + " " + Str$(cycles) + " */"
            End If
        Else          'execute command
```

```
                  If command = "wait" Then
                      cycles = cycles - 1
                  ElseIf command = "up" Or command = "down" Then
                      cycles = cycles - Abs(Asc(Mid(holdover, 4, 1)) - Asc("0"))
                  End If
           End If
       End If

If recordflag Then
     Print #3, Str$(capdata) + " " + Str$(zygodata) + " " + Str$(picodata) + " " +
Str$(tempdata) + " " + caldata
End If

End Sub
Private Sub decodezygo()
' decode position in units of nanometers, display on strip chart
     zygodata = (Val(holdzygo) * 632.991501) / (1.000271296 * 512)
End Sub
Private Sub picogo_Click()
If Val(picosteps.Text) > 0 And Val(picosteps.Text) < 2001 Then
     Call runpico(Val(picosteps.Text), CW.Value)
Else
     Call MsgBox("Invalid step number!", vbOKOnly)
End If
End Sub
Private Sub runpico(numsteps As Integer, picocw As Boolean)

Dim step1 As Integer
Dim step2 As Integer
step1 = Val(numsteps) \ 256
step2 = Val(numsteps) Mod 256
If picocw = True Then
     MSComm1.Output = "C" + Chr$(step1) + Chr$(step2) + "X"
Else
     MSComm1.Output = "D" + Chr$(step1) + Chr$(step2) + "X"
End If
End Sub

Private Sub programmed_Click()
programmed.Value = True
continuous.Value = False
Frame1.Enabled = True
Record1.Enabled = False
picoframe.Enabled = False
End Sub

Private Sub Record1_Click()
Dim tmpFN As String
Dim temp As String

If Record1.Caption = "Record" Then
     On Error GoTo ErrHandler
     CommonDialog1.Filter = "All Files (*.*)|*.*|Text Files (*.txt)|*.txt|Dat Files
(*.dat)|*.dat|"
     CommonDialog1.FilterIndex = 1
     CommonDialog1.ShowSave
     tmpFN = CommonDialog1.FileName
     Open tmpFN For Output As #3
'      Close #3
'      Open tmpFN For Append As #3
     Record1.Caption = "Save Log"
     RecordLight.Visible = True
     RecordLabel.Visible = True

     Print #3, "/* Record starting at " + Str$(Now) + "*/"        'insert time stamp
     recordflag = True
Else
     recordflag = False
     Record1.Caption = "Record"
     RecordLight.Visible = False
     RecordLabel.Visible = False
```

```
      Print #3, "/* Halted at " + Str$(Now) + "*/"
      Close #3

End If
ErrHandler:
MSComm1.InputLen = 0
temp = MSComm1.Input
MSComm2.InputLen = 0
temp = MSComm1.Input
End Sub
Private Sub reset_Click()
Dim temp As String
holdover = ""
Timer1.Interval = 50
Record1.Enabled = True
CW.Value = True
CCW.Value = False
numerror = 0
picodata = 0

MSComm1.Output = "*"          'reset communications with TI microprocessor
MSComm1.InputLen = 0
temp = MSComm1.Input
MSComm2.InputLen = 0
temp = MSComm2.Input

End Sub
Private Sub resetzygo_Click()
      MSComm2.Output = "RESTART" + Chr$(10) + Chr$(13)
      If recordflag Then
            Print #3, "/* Reset Zygo */"
      End If
End Sub

Private Sub startdaq_Click()
Dim errorfound As Boolean

errorfound = False
scriptbuf = script.Text + Chr$(13)
If Len(scriptbuf) <= 2 Then
      errorfound = True
End If

Do Until Len(scriptbuf) <= 2
      delimiter = InStr(scriptbuf, " ")
      If delimiter = 0 Then
            errorfound = True
      Else
            command = Mid$(scriptbuf, 1, delimiter - 1)
      End If
      Select Case command
            Case Is = "up"
            Case Is = "down"
            Case Is = "wait"
            Case Is = "temp"
            Case Else
                  errorfound = True
      End Select
      scriptbuf = Mid$(scriptbuf, delimiter + 1, Len(scriptbuf))
      delimiter = InStr(scriptbuf, Chr$(13))
      If delimiter = 0 Then
            errorfound = True
      End If
      cycles = Val(Mid$(scriptbuf, 1, delimiter - 1))
      If cycles < 0 Or (command = "up" And cycles >= 2000) Or _
            (command = "down" And cycles >= 2000) Or cycles >= 50000 Then
            errorfound = True
      End If

      scriptbuf = Mid$(scriptbuf, delimiter + 2, Len(scriptbuf))
```

88

```
Loop

If errorfound Then
    Call MsgBox("Error found in script!" + Chr$(13) + "Did not execute.", vbOKOnly)
Else    'parse the first one
    scriptbuf = script.Text + Chr$(13)
    delimiter = InStr(scriptbuf, " ")
    command = Mid$(scriptbuf, 1, delimiter - 1)
    scriptbuf = Mid$(scriptbuf, delimiter + 1, Len(scriptbuf))
    delimiter = InStr(scriptbuf, Chr$(13))
    cycles = Val(Mid$(scriptbuf, 1, delimiter - 1))
    scriptbuf = Mid$(scriptbuf, delimiter + 2, Len(scriptbuf))
    Select Case command
        Case Is = "up"
            Call runpico(cycles, False)
        Case Is = "down"
            Call runpico(cycles, True)
        Case Is = "temp"
            MSComm1.Output = "T"
            cycles = 0
        Case Else
    End Select
    Frame1.Enabled = False
    picoframe.Enabled = False
    scriptflag1 = True
    startdaq.Caption = "Running Script..."
    startdaq.Enabled = False
    Open savefilename For Output As #3
    Close #3
    Open savefilename For Append As #3
    Print #3, "/*Record starting at " + Str$(Now) + "*/"        'insert time stamp
    Print #3, "/*" + Chr$(13) + scriptbuf; Chr$(13) + "*/"
    recordflag = True
End If

End Sub

Private Sub Timer1_Timer()

MSComm2.Output = "R? 2,M" + Chr$(10) + Chr$(13)

End Sub
```

Appendix F: Matlab Data Analysis and Graphing Code

```
function cap_baseline_long3=cap_baseline_long3(file)
%data processing routine and graphing routine for nanogate capacitance sensor
%with calibration values
%Jan. 16, 2004
%Hongshen Ma hongma@mit.edu

%variable assignments:
%capraw - raw data from capacitance measurement
%zygo - raw data from zygo
%pico - pico motor data
%temp - temperature
%cal - calibration indicator. 0=normal operation, 1=calibration value
%cap - capacitance data with the calibration data points removed and pitted with the
previous data value
%caled - capacitance with calibration value subtracted
%calpoints - number of data points taken for each calibration
%caldata - array of all the calibration points

%*** we assume the first data point is not a calibration point

calendpoint=1;
[capraw, zygo, pico, temp, cal] = textread(file, ' %f %f %d %f %f %*[^\n]',
'headerlines', 1, 'commentstyle', 'c');

caldata=[];
cap=capraw;
caled=capraw;
i=1;
while not(cal(i)==1)
    i=i+1;
end
calbuf=mean(capraw(i+1:calend(cal, i)-1));
i=1;
while i<=length(capraw)
    if cal(i)==1
        calendpoint=calend(cal, i);
        calbuf=mean(capraw(i+1:calendpoint-1));   %for calibration we also don't use the
last datapoint
        caldata=[caldata calbuf];
        cap(i:calendpoint)=cap(i-1);           %pad over calibration data point
        caled(i:calendpoint)=caled(i-1);    %but we don't use the one datapoint right
before the calibration
        i=calendpoint+1;
    else
        caled(i)=caled(i)-calbuf;
        i=i+1;
    end
end

timeaxis=1:1:length(cap);
timeaxis = timeaxis ./ (2.5*3600); %hours
%timeaxis = timeaxis ./ (2.5); %seconds
capnm=(cap-mean(cap))*450/2e6;
calednm=(caled-mean(caled))*450/2e6;
caldatanm=(caldata-mean(caldata))*(450/2e6);
voltage=(cap-mean(cap))*(2.5/(2^24))*1e6;

std(capnm)
std(calednm)

figure; plot(timeaxis, capnm, 'k-');
title(strcat('Capacitive sensor long term drift (file: ', file, ')'), 'fontsize', 10);
ylabel('Capacitively measured displacement (nm)', 'fontsize', 11);
xlabel('Time (hours)', 'fontsize', 11);
%figure; plot(timeaxis, temp);
%title(strcat('Temperature Fluctuation (file: ', file, ')'), 'fontsize', 10);
%ylabel('Temperature (degrees C)', 'fontsize', 10);
%xlabel('Time (hours)', 'fontsize', 10);
```

```matlab
figure; plot(temp, capnm);
title(strcat('Position vs. Temperature (file: ', file, ')'), 'fontsize', 10);
ylabel('Displacement (nm)', 'fontsize', 10);
xlabel('Temperature (degrees C)', 'fontsize', 10);
figure; plot(timeaxis, capnm, 'c:', timeaxis, calednm, 'k-');
title(strcat('Calibrated capacitive data (file: ', file, ')'), 'fontsize', 10);
ylabel('Calibrated displacement measurement (nm)', 'fontsize', 10);
xlabel('Time (hours)', 'fontsize', 10);


function [calend]=calend(indicators, startpoint)
endpoint=startpoint;
while (indicators(endpoint)==1)
    endpoint = endpoint + 1;
end
endpoint=endpoint-1;
calend=endpoint;

function startingpoint=startpoint(file)
%data processing and graphing routine for nanogate
%written by Hong Ma
%Sept. 22, 2003

[cap, zygo, pico, temp, cal] = textread(file, ' %f %f %d %d %s', 'headerlines', 1,
'commentstyle', 'c');
timeaxis=1:1:length(cap);
timeaxis = timeaxis ./ 125;

zygolength=fix(length(cap)/4);
for i=1:zygolength
    zygotemp(i)=zygo(i*4);
end
zygointerp=[interp(zygotemp, 4) zygotemp(zygolength)]; %pad one extra data point

cap_up=[]; cap_down=[]; cap2=[]; cap3=[]; zygo_up=[]; zygo_down=[]; zygo2=[]; zygo3=[];
for i=1:4100
    if cap(i)>=7000000 & cap(i)<=9000000
        cap_up(length(cap_up)+1)=cap(i);
        zygo_up(length(zygo_up)+1)=zygointerp(i);
    elseif cap(i)<7000000 & cap(i)>6600000
        cap2(length(cap2)+1)=cap(i);
        zygo2(length(zygo2)+1)=zygointerp(i);
    elseif cap(i)>6450000 & cap(i)<=6600000
        cap3(length(cap3)+1)=cap(i);
        zygo3(length(zygo3)+1)=zygointerp(i);
    end
end
for i=4100:length(cap)
    if cap(i)>=7000000 & cap(i)<=9000000
        cap_down(length(cap_down)+1)=cap(i);
        zygo_down(length(zygo_down)+1)=zygointerp(i);
    elseif cap(i)<7000000 & cap(i)>6600000
        cap2(length(cap2)+1)=cap(i);
        zygo2(length(zygo2)+1)=zygointerp(i);
    elseif cap(i)>6450000 & cap(i)<=6600000
        cap3(length(cap3)+1)=cap(i);
        zygo3(length(zygo3)+1)=zygointerp(i);
    end
end

x1=[6600000 6600000];
y1=[-100, 500];
x2=[7000000 7000000];
y2=[-100, 500];
figure; plot(cap_up, zygo_up, 'b', cap2, zygo2, 'g', cap3, zygo3, 'r', x1, y1, 'k-', x2,
y2, 'k-');
title(strcat('Zygo vs. Capacitance (file: ', file, ')'), 'fontsize', 12);
xlabel('Capacitance (ADC counts)', 'fontsize', 12);
ylabel('Zygo readout (nm)', 'fontsize', 12);
a=polyfit(cap_up, zygo_up, 1);
baseline=mean(zygo3)
```

```
(baseline-a(2))/a(1)
x3=[6000000 9000000];
y3=[baseline baseline];
x4=[6400000 9000000];
y4=a(1)*x4+a(2);
figure; plot(cap_down, zygo_down, 'b', cap2, zygo2, 'g', cap3, zygo3, 'r', x1, y1, 'k-',
x2, y2, 'k-', x3, y3, 'r-', x4, y4,'r-');
title(strcat('Zygo vs. Capacitance (file: ', file, ')'), 'fontsize', 18);
xlabel('Capacitance (ADC counts)', 'fontsize', 16);
ylabel('Zygo readout (nm)', 'fontsize', 16);

%residue plot
capresidue_up=zygo_up-(a(1)*cap_up+a(2));
capresidue_down=zygo_down-(a(1)*cap_down+a(2));
figure; plot(cap_up, capresidue_up, 'b-', cap_down, capresidue_down, 'r:');
title(strcat('Residue from Zygo vs. Capacitance (file: ', file, ')'), 'fontsize', 12);
xlabel('Capacitance (ADC counts)', 'fontsize', 12);
ylabel('Zygo readout (nm)', 'fontsize', 12);
legend('Opening', 'Closing', 0);
```